LGR5 has been reported to be upregulated in several tumors. We have previously shown that expression of LGR5 in the noncancerous liver was very low, however LGR5 is frequently overexpressed in hepatocellular carcinoma (HCC) with β-catenin mutations [6]. Although mutations of β-catenin are found in nearly 40% of HCC, the LGR5 has not been reported as the marker of hepatocyte, nor mentioned as a marker gene for liver regeneration. LGR5 also has been identified as a gene responsible to promote cell proliferation and tumor formation in basal cell carcinoma (BCC), a common malignant tumor of the skin [7]. High levels of LGR5 expression were also reported in colon and ovarian carcinomas [8], and we have shown that a high level of LGR5 expression in colorectal cancer was significantly correlated with tumor stage [9]. One study using colorectal cancer cell lines showed that suppression of LGR5 expression enhances tumorigenesis and is linked to a more mesenchymal phenotype [10].

There are some evidences suggest that LGR5 is a downstream target gene of Wnt signaling pathway [2,6,11,12]. The Wnt signaling pathway comprises a vast number of protein interactions and plays a critical role in morphogenesis and tumorigenesis. To date, three main pathways related to Wnt signaling have been identified: the β-catenin-dependent, planar cell polarity, and Wnt/$Ca^{2+}$ pathways [13]. The β-catenin-dependent pathway, otherwise known as the canonical pathway, has been the most intensively studied. Mutations or deletions in AXN1/2 or APC genes inhibit the phosphorylating activity of GSK-3β, thereby stabilizing cytoplasmic β-catenin, and provoking aberrant cellular gene expression. Mutations at sites that affect β-catenin phosphorylation also cause cytoplasmic accumulation of β-catenin and lead to dysregulation of the pathway. Recently, LGR5 was reported to be a receptor of R-spondins which were known to be a potent family protein mediating Wnt/β-catenin and Wnt/PCP signaling [11,12,14]. Acquirement of stem cell-like properties in various tumors have greatly increased the possible role of these cells in tumorigenesis [15,16]. Upregulation of LGR5 in several tumors with increased Wnt signaling pathway suggests the possible role of LGR5 gene in oncogenesis and morphogenesis [6–9]. However, the functional role of LGR5 in tumor cells is still poorly understood. In this study, we aimed to analyze the function of LGR5 in hepatocellular carcinoma cells.

## Materials and methods

### Cell culture and chemicals

Cells were cultured in RPMI 1640 supplemented with 10% fetal bovine serum, 100 U/ml of penicillin and 100 μg/ml of streptomycin [6,9]. HepG2 containing a deletion of exon 3 of the β-catenin gene and PLC/PRF/5 containing a deletion of exon 4 of the AXIN1 were used as cell lines with activated Wnt signaling and high levels of LGR5 mRNA[17]. KYN2 cells were used as a cell line with low expression of LGR5 mRNA [6,9].

### Plasmids, transfection, and establishment of stable transfectants

A FLAG-tagged LGR5 expression vector (LGR5-FL) was constructed by inserting the full-length coding cDNA for human LGR5 (RZPD, Berlin, Germany) into the Bgl II site of p3XFLAG-CMV-14 (Sigma-Aldrich, St. Louis, MO, USA). KYN-2 cells were transfected with LGR5-FL or empty vector using Lipofectamine LTX reagent (Invitrogen, Carlsbad, CA, USA). Production of LGR5-FL protein was detected by confocal laser scanning microscopy (LSM510, Carl Zeiss, Germany) and western blot analysis, using the FLAG M2 antibody (Sigma-Aldrich). F-actin was stained with TexasRed X-phalloidin (Molecular Probes, Eugene, OR, USA) and nucleus was stained with VECTASHIELD Mounting Medium with DAPI (Vector Laboratories Inc. Burlingame, CA, USA). Anti-E-cadherin (ALX-804-201-C100, Enzo Life Sciences, Inc.) and anti-β-catenin (E-5, Santa Cruz Biotechnology, Inc.) antibodies were used for immunofluorescent staining. Colonies that formed in 0.3% soft agar medium containing G418 (Invitrogen) were picked and propagated. Each colony was purified by three sequential series of limiting dilutions. Ultimately, six LGR5-transfected clones (KY-B1, KY-G1, KY-G2, KY-G6, KY-F3, and KY-S1) and five empty vector-transfected clones (KY-V2, KY-V3, KY-V4, KY-V5, and KY-V6) were established. Protein levels were analyzed by western blotting and mRNA levels were analyzed by quantitative PCR. Canonical Wnt signaling activity was measured with the TCF-luciferase reporter system (TOPflash/FOPflash, Upstate Millipore Co.), and the results are shown as the ratio of TOPflash to FOPflash (TOP/FOP).

### Quantitative polymerase chain reaction (qPCR)

Total RNA was isolated from cells using the RNeasy Mini Kit, including DNase treatment (Qiagen KK, Tokyo, Japan). cDNA was synthesized using the PrimeScript® RT reagent kit (Perfect Real Time; Takara Bio, Shiga, Japan), and qPCR was performed on a Thermal Cycler Dice Real Time System using SYBR *Premix Ex Taq*™ (Perfect Real Time; Takara Bio). The primer sequences for qPCR were as follows: GAPDH forward, 5′–ATCATCCCTGCCTCTACTGG-3′; GAPDH reverse, 5′–TTTCTAGACGGCAGGTCAGGT-3′; LGR5 forward, 5′–GAGGATCTGGTGAGCCTGAGAA-3′; LGR5 reverse, 5′–CATAAGTGATGCTGGAGCTGGTAA-3′; RSPO1 forward, 5′–AAGGCTGTGAGCTCTGCTCT-3′; RSPO1 reverse, 5′–ATGTCGTTCCTCTCCAGCAG3′. GAPDH was used as a reference. Fold induction values were calculated using the $2^{-\Delta\Delta\ Ct}$ method. All experiments were performed in triplicate and repeated at least three times in separate experiments; representative data are shown.

### Cell proliferation, cell migration, and cytotoxicity assays

Cells were plated in 24-well dishes, and the number of cells was counted in a hemocytometer after staining with trypan blue. Ratio number of cells represents the total mean number of LGR5-overexpressing cells or empty vector cells for each day compared to the total mean number of cells at day 0. RNA interference experiments were performed using siRNA. The target sequences were as follows: LGR5-585, 5′–GAA CAA AAU ACA CCA CAUA-3′; LGR5-662, 5′–GAA UCC ACU CCC UGG GAAA-3′. AllStars Negative Control siRNA (Qiagen) was used as a control. Cells were transfected with the final concentration of 10 nM siRNA using Lipofectamine RNAiMAX transfection reagent (Invitrogen).

For cytotoxicity tests, cells were treated with puromycin for 20 h, washed with PBS and covered with growth medium containing 0.3% agar. Cells were cultured for 2 weeks with occasional replenishment of the medium. Colonies were stained

with nitro blue tetrazolium reagent and photographed for counting. For cell migration assays, cells were placed in six-well dishes and incubated for two days. The confluent monolayer cultures were scratched and photographed after 24 h. The width of each scratch was measured at ten points and more than five scratches were measured for each group. For RNA interference assays, cells were transfected with siRNAs for 20 h and replated in six-well dishes. The monolayer cultures that formed 24 h later were scratched and photographed as described previously.

### Tumor formation assays

Clones containing LGR5-FL or empty vector were transplanted into the subcapsular region of the livers of NOG mice (NOD/Shi-scid/IL-2γ−/−) at $5 \times 10^6$ cells per mouse. The tumors that formed in the liver were resected, fixed with 10% neutral-formalin, and used for histological analysis. For metastasis assays, cells were inoculated into the subcapsular region of the spleens of NOG mice, and tumors that formed in the liver were used for histological analysis.

### Statistical analysis

Differences were assessed for statistical significance using Student's *t*-test, with the level of significance being $P<0.05$.

## Results

### Establishment of LGR5-overexpressing clones

To determine the function of LGR5 in cancer cells, stable clones containing the LGR5 gene were established. We have tested several commercially available anti-LGR5 antibodies, however, we could not obtain good results in order to detect LGR5 protein expression in HCC tissue. Thus, we constructed a FLAG-tagged LGR5-expression vector (LGR5-FL), and production of the protein was detected by immunofluorescence microscopy and western blot analysis using anti-FLAG antibody. When LGR5-FL was transfected into KYN-2 cells, the protein was localized mostly in the cytoplasm and cytoplasmic membrane (Fig. 1A). To establish stable clones, LGR5-FL or empty vector was transfected into KYN-2 cells, and G418-resistant colonies that formed in soft agar medium were purified by three series of limiting-dilution propagations. Six clones stably transfected with LGR5-FL (KY-B1, KY-G1, KY-G2, KY-G6, KY-F3, KY-S1) and five clones stably transfected with empty vector (KY-V2, KY-V3, KY-V4, KY-V5, KY-V6) were isolated. The LGR5 protein (~100 kD) was detected by western bot analysis (Fig. 1B), and mRNA levels were measured by qPCR (Fig. 1C). The KY-G1 and KY-S1 transfectants expressed high levels of LGR5 protein and mRNA. The protein and mRNA levels in each of the clones were well correlated, and the same levels were maintained after several passages. Only the results for three vector-transfectants are shown in Fig. 1B and C, but the other clones showed similar results.

Phase contrast microscopy showed that LGR5-overexpressing KY-G1 and KY-S1 cells had a round shape and aggregated together, whereas KY-V2 and KY-V3 cells had a flat extended shape and spread on the culture dishes (Fig. 1D). LGR5-transfectants stacked up on the surface of the culture dishes, whereas empty vector–transfectants formed flat monolayers (Fig. 1E). Phalloidin staining showed strong F-actin signals between KY-G1 cells (so-called cortical actin), whereas KY-V2 cells showed a flat extended shape with F-actin in the cytoplasm (Fig. 1F). Distinct fluorescent signals of E-cadherin were located between KY-G1 cells (Fig. 1G). Similar distribution of β-catenin was also seen in KY-G1 and KY-V2 cells, respectively (Fig. 1H). Accumulation of β-catenin in nuclei which is often seen in cell with activated Wnt signaling could not be detected in LGR-5 overexpressing KY-G1 cells. Non-adherent cultures of KY-G1 cells formed spherical shapes and most of the cells in the center survived intact, whereas KY-V2 cells formed irregular spheres and some of these had a necrotic area at the center (Fig. 1G).

### Overexpression of LGR5 promotes HCC cell viability, enhances colony formation, and decreases cell motility

The rates of proliferation of KY-G1 and KY-V2 cells were identical until cell numbers reached a maximum, however, KY-G1 cells survived longer in overgrowth conditions (Fig. 2A). Substantial numbers of KY-G1 cells survived after two weeks in overgrowth culture, whereas KY-V2 cells detached from the surface of the dishes and only a small proportion of cells survived in over-growth culture (Fig. 2B). In addition, KY-G1 cells were more resistant to the toxicity of puromycin (Fig. 2C), and also formed soft agar colonies more efficiently than KY-V2 cells (Fig. 2D). The motility of the cells was measured by performing scratch tests on confluent cell cultures. Retardation of cell migration was observed as early as 5 h in KY-G1 cells (data not shown), and scratch scars were repaired more rapidly at 24 h in KY-V2 cell cultures than in KY-G1 cell cultures (Fig. 2E). The reduction ability of LGR5-overexpressing cells to migrate after scratch wound assay was also previously reported in colorectal carcinoma cell lines [10].

### LGR5-overexpressing HCC cells forms nodular tumors with decreased infiltration and metastatic foci

To further evaluate the function of LGR5 in vivo, KY-G1 or KY-V2 cells were transplanted into the subcapsular region of the livers of NOG mice. KY-G1 cells formed tumors with trabecular pattern in the liver, while KY-V2 cells formed tumors with ill trabecular pattern (Fig. 3A a, b). Expression of LGR5-FL was detected in the tumors formed by KY-G1 cells but not in the tumors formed by KY-V2 cells (Fig. 3A a, b inserts). Reticulum staining showed a trabecular pattern in the KY-G1 tumors, whereas a solid pattern was observed in the KY-V2 tumors (Fig. 3A c, d). Infiltration into the vicinal muscle tissues was rare in the tumors formed by KY-G1 cells, but occasionally seen in the tumors formed by KY-V2 cells (Fig. 3A e, f). When KY-G1 cells were transplanted into the subcapsular region of the spleen, the number of metastatic foci in the liver, and the number of micrometastases into the portal veins was lower, compared with transplantation of KY-V2 cells (Fig. 3B a–c). In addition, tumors formed by KY-V2 cells showed a wider area of hemorrhagic necrosis compared with those formed by KY-G1 cells.

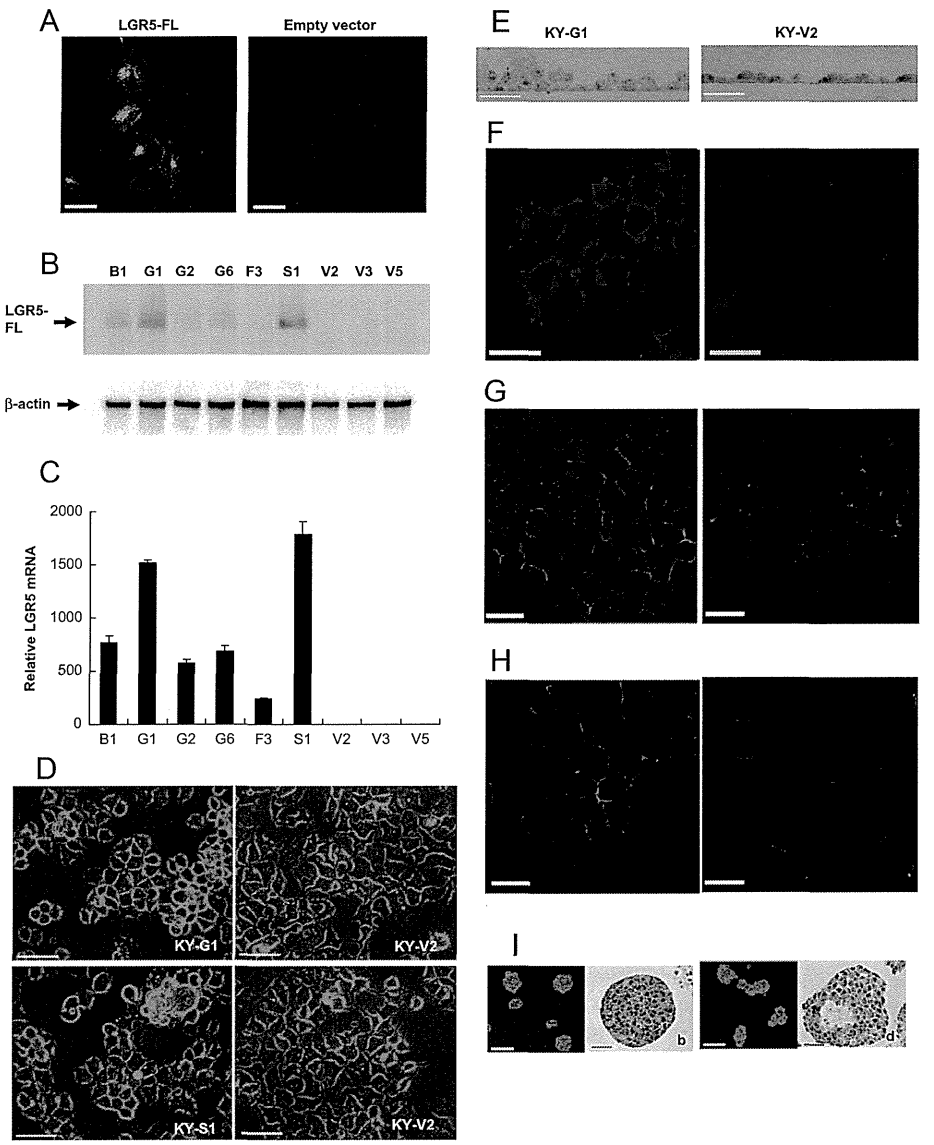


**Fig. 1 – Establishment of LGR5-overexpressing clones. A: Immunofluorescent staining of KYN-2 cells transiently transfected with LGR5-FL or empty vector. Cells were stained with anti-FLAG antibody. Green: LGR5. Red: F-actin. Blue: nuclei. Bar, 50 μm. B: Western blot analysis of LGR5-overexpressing clones (KY-B1, KY-G1, KY-G2, KY-G6, KY-F3, KY-S1). KY-V2, KY-V3 and KY-V5 were stable transfectants containing empty vector. Blots were stained with anti-FLAG antibody (upper) or anti-β-actin antibody (lower). C: Expression of LGR5 mRNA in stable transfectants. Relative LGR5 mRNA level was shown as fold increase when the average level of non-transfected KYN-2 was set at 1. D: Morphology of clones containing LGR5-FL (KY-G1 and KY-S1) or empty vector (KY-V2 and KY-V3). (Bar, 100 μm) E: Vertical sections of 3-day cultures. KY-G1 and KY-V2 cells were embedded in EPON resin and sliced sections were stained with toluidine blue. F: Distribution of F-actin. F-actin was visualized by staining with phalloidin. Bar, 100 μm. G: Localization of E-cadherin (Green: E-cadherin, Blue: nuclei, Bar, 50 μm). H: Localization of β-catenin (Green: E-cadherin, Blue: nuclei, Bar, 50 μm). I: Morphology of non-adherent cultures of KY-G1 (a, b) and KY-V2 (c, d). Photographs show phase contrast microscopy (a, c. Bar, 200 μm) and HE staining of paraffin embedded sections (b, d. Bar, 500 μm). E-I: KY-G1 (left column), KY-V2 (right column). (For interpretation of the references to color in this figure, the reader is referred to the web version of this article.)**

### Down-regulation of LGR5 in HCC cells transforms cells to a loosely associated morphology and increased cell motility

To determine whether the characteristics of the KY-G1 cells were indeed due to the expression of higher levels of LGR5, we examined the effect of down-regulating LGR5 using siRNA. HepG2 cells were transfected with two siRNA sequences (si585 and si662) and LGR5 mRNA levels were analyzed by qPCR. LGR5 mRNA levels were significantly decreased 24–96 h after transfection of siRNAs against LGR5 (Supplementary Fig. 1; only 48 h data is shown). si662 suppressed expression of LGR5 more efficiently than si585, and similar results were obtained with

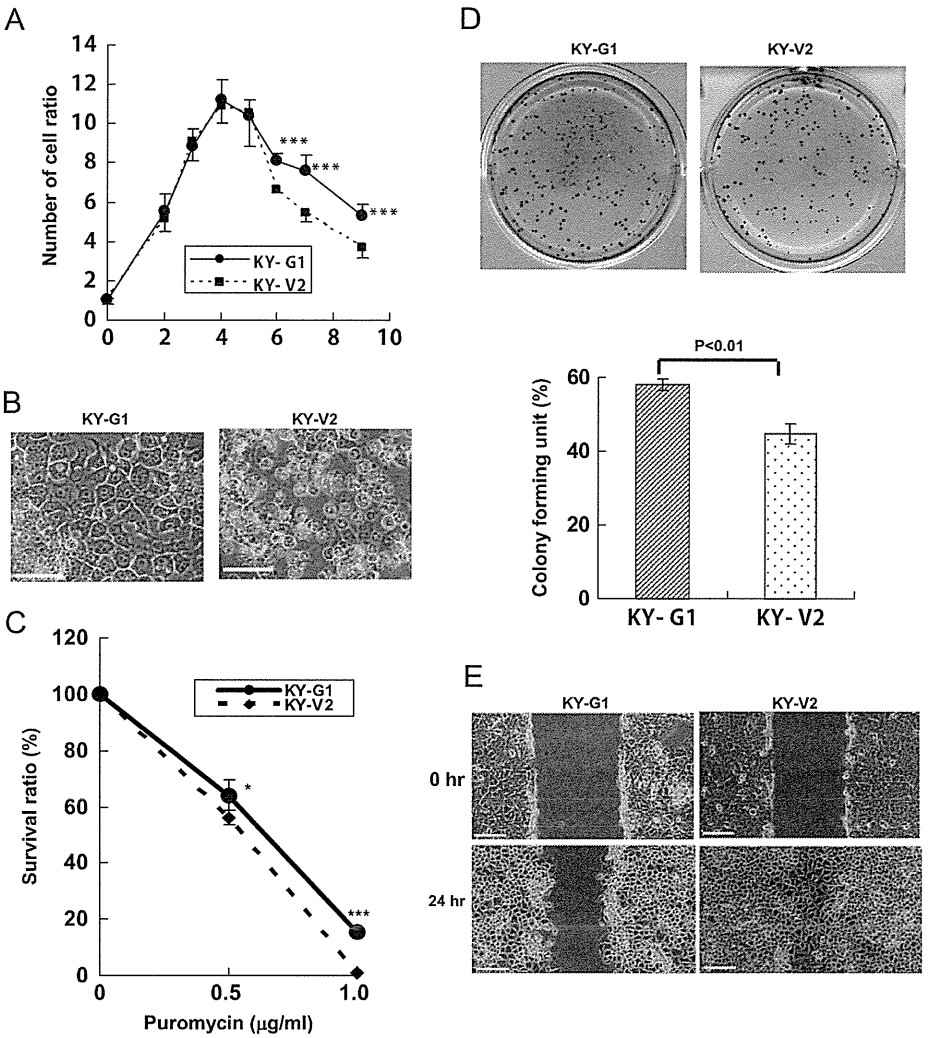


**Fig. 2 – Characterization of LGR5-overexpressing clones. A: Growth and survival of KY-G1 and KY-V2 cells. High levels of LGR5 expression did not affect the growth rate of the cells; however, KY-G1 cells survived longer in overgrowth conditions. ***: $P<0.01$. B: Morphology of clones after 2 weeks of culture. (Bar, 100 μm) Viable cells were still observed in the KY-G1 culture, but few cells were alive in the KY-V2 culture. C: Resistance to cytotoxicity. Cells were treated with puromycin for 20 h, and cultured under soft agar medium. Cells with high expression of LGR5 were more resistant to the cytotoxic effect of puromycin. *: $P<0.05$. ***: $P<0.01$. D: Colony formation. Upper: 500 cells were cultured in soft agar plates for 2 weeks. Lower: quantitative assay of colony forming activity. Colony forming unit: ratio of colonies formed to number of cells inoculated (%). High levels of LGR5 expression enhanced colony formation. E: Motility assay. Confluent cell layers were scratched and photographed at 0 and 24 h. High levels of LGR5 expression inhibited cell motility. (Bar, 200 μm).**

PLC/PRF/5 cells (Supplementary Fig. 2). When LGR5 mRNA was down-regulated with siRNA, the tight aggregated morphology of HepG2 cells was transformed to a loosely associated morphology. Some of the cells began to migrate away from the cell aggregates (Fig. 4A, upper column). The strongly staining cortical actins between the cells became extended filaments when expression of LGR5 was down-regulated (Fig. 4B, upper column). siRNA directed against LGR5 showed similar effects in PLC/PRF/5 cells (Fig. 4A and B, lower columns). The cortical actin between the cells became long, extended filaments. Down-regulation of LGR5 also increased cell motility. When HepG2 cells were treated with si585 or si662, scratched scars were repaired more rapidly than in cells treated with siControl (Fig. 5A, C). Similar results were obtained when PLC/PRF/5 cells were treated with siRNA directed against LGR5 (Fig. 5B, C).

## Discussion

To determine the function of LGR5 in tumor cells, we carefully investigated cell clones containing a FLAG-tagged expression vector (LGR5-FL). The LGR-5 transfected clone (KY-G1) became rounded and formed aggregates when grown as an adherent culture. It formed spherical bodies when propagated in suspension culture, more resistance to cytocidal conditions, and showed decreased migratory activity. The Wnt signaling pathway is an

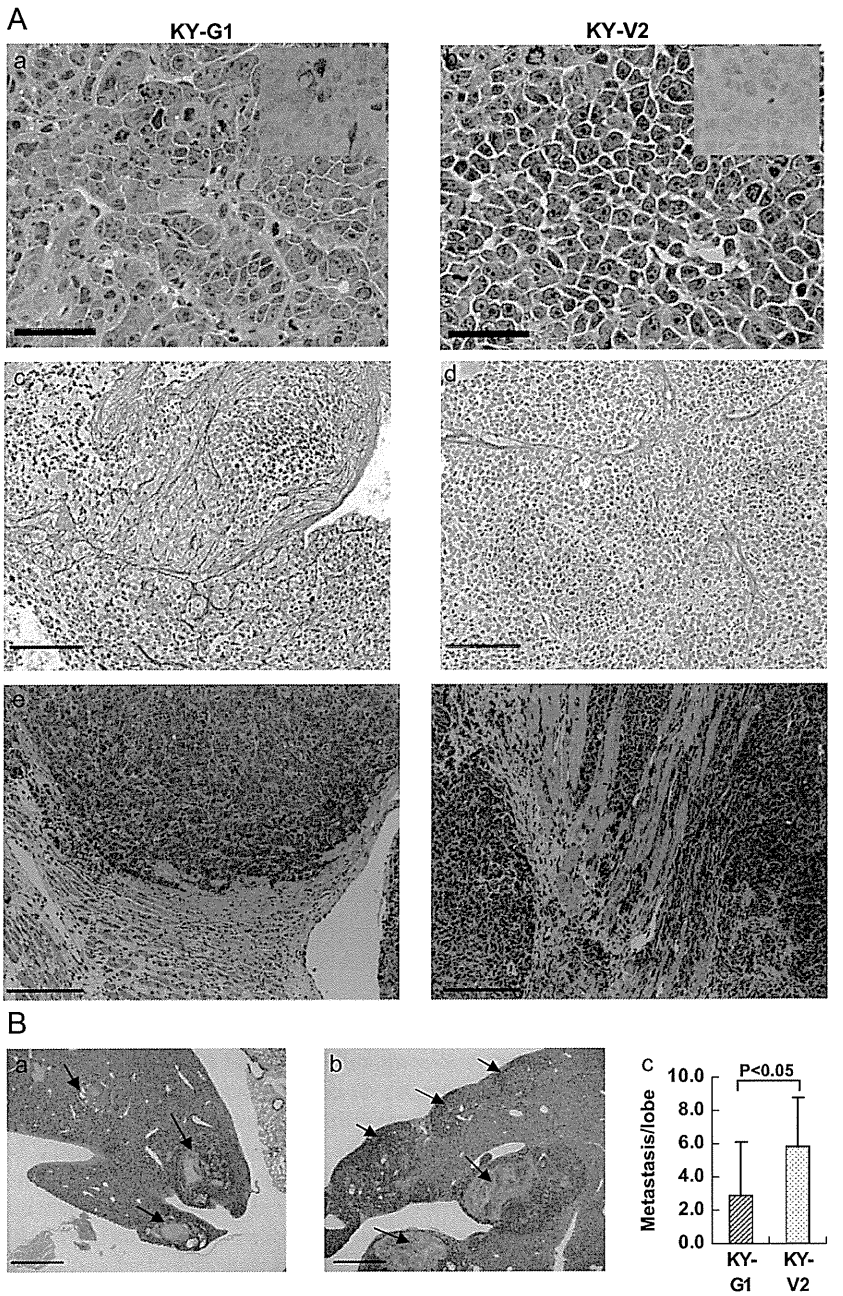


**Fig. 3 – Histological analysis of tumors formed by KY-G1 or KY-V2 clones in the livers of NOG mice. A: KY-G1 (left) and KY-V2 (right) cells were transplanted into the subcapsular region of the livers of mice. Tumors were resected and thin sections were stained with HE (a, b. Bar, 100 μm)(e, f. Bar, 200 μm) or silver impregnation (c, d. Bar, 200 μm). Inserts show immunohistochemical staining with anti-FLAG antibody (a, b). B: KY-G1 (a) and KY-V2 (b) cells were transplanted into subcapsular region of the spleens of NOG mice. Tumors that formed in the livers were fixed and stained with HE (Bar 500 μm). Arrows show metastatic foci in the liver. The number of metastases was quantified (c). Tumors larger than 0.25 mm in diameter were counted. High levels of LGR5 expression inhibited metastasis to the liver.**

important pathway for morphogenesis and maintaining the stemness of cells. Sphere formation, colony formation and resistance to cytotoxic drugs are important criteria for the stemness of cells. LGR5-overexpressing KY-G1 cells formed tightly packed spheres, with viable cells extending from the surface to the center when cultured under non-adherent conditions, whereas KY-V2 cells containing the empty vector formed loose, irregular spheres, and some cells in the central area showed signs of necrosis. KY-G1 cells were also more resistant to a cytocidal environment, survived longer under nutrient depletion conditions, and were more resistant to the cytocidal effect of puromycin. The differences between LGR5-transfected and vector-transfected cells were rather marginal, which may be affected by the

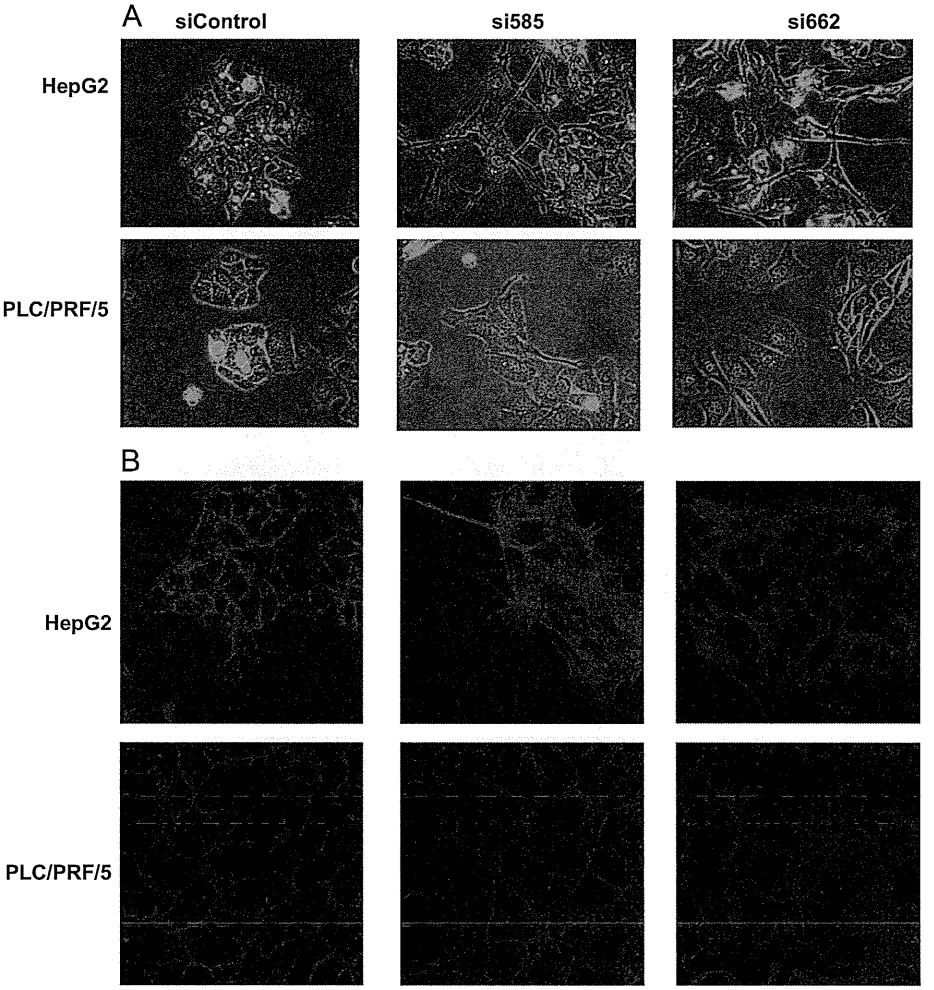


**Fig. 4 – Down-regulation of LGR5 in HCC cell lines by treatment with siRNAs. HepG2 and PLC/PRF/5 cells were transfected with siControl, si585 or si662, and cultured for 2 days. A: Phase contrast microscopy. ( × 400) B: Immunofluorescent microscopy. Actin filaments were stained with phalloidin. ( × 400).**

presence of substantial expression of LGR4 in parental KYN-2 cells. LGR4, LGR5, and LGR6 have homology with about 50% identity between each other at the amino acid level, and may compensate each other functions [18]. Since LGR4 is constitutively expressed in most kind of cells, we assumed that the results is more meaningful if we could obtain a difference between LGR5-overexpressing cells compared to the control empty vector cells, even though it is marginal. Moreover, we observed that parental KYN-2 cells had already reached the stage of anchorage-independent growth, while, a high level of LGR5 expression enhanced colony formation. This could be explained by high levels of LGR5 conferring resistance to cell death, and enhancing cell survival when they were scattered as single cells in the soft agar medium. KY-G1 cells aggregated and stacked up when cultured on the surface of the dishes, which consequently made them migrated slower than KY-V2 cells. These findings may explain why HCC is generally resistant to antitumor drugs used in chemotherapy. Many proteins related to the Wnt signaling pathway have been reported to modulate the actin–cytoskeleton structure. The frizzled/disheveled pathway controls the planar polarity of cells. Adenomatous polyposis coli (APC) protein is transported along microtubules, and regulates the cytoskeleton and cell migration [19]. β-catenin, a crucial transcription factor in the Wnt pathway, links E-cadherin with α-catenin to form firm adhesive junctions. LGR5, which is regarded as a target gene of the Wnt signaling pathway, quite possibly contributes to changes in cell morphology. Down-regulation of LGR5 in HepG2 and PLC/PRF/5 cells resulted in the cells acquiring a flat shape, with loss of cortical actin and migration of cells away from the aggregates. It also transformed HCC cells into a loosely associated morphology and increased cell motility. Reversely, high levels of LGR5 expression cells formed spherical shapes where most of the cells gathered intactly to the center. These results suggest that high levels of LGR5 expression affect epithelial cell morphology and confer some of the properties of stem cells on tumor cells.

To investigate the function of LGR5 in vivo, KY-G1 cells were orthotopically transplanted into NOG mice. KY-G1 cells formed nodular tumors typical of hepatocellular carcinomas, whereas the tumors formed by KY-V2 cells were diffuse and occasionally infiltrated into the contiguous tissues. Moreover, KY-V2 cells formed more micrometastases in the liver when implanted into the subcapsular region of the spleen. We previously categorized HCC cell lines into two groups; one highly metastatic and the

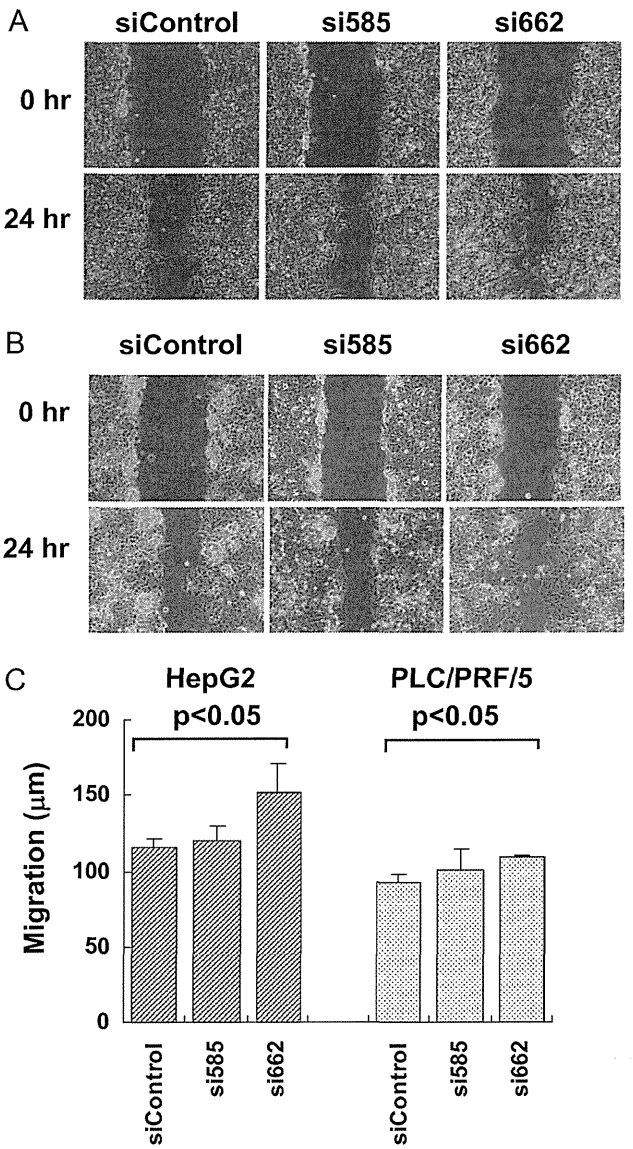


**Fig. 5 – Motility of HCC cells after down-regulation of LGR5. Cells transfected with siControl, si585, or si662 were cultured for 2 days. Cell monolayers were scratched and photographed at 24 h. A: HepG2. B: PLC/PRF/5. C: Migration distance.**

other non-metastatic [20]. It is quite interesting that KYN-2 and Li7 which express low levels of LGR5 were categorized as highly metastatic, whereas HepG2 and PLC/PRF/5 which express high levels of LGR5 were categorized in the non-metastatic group. Our previous clinicopathological study also showed that overexpression of LGR5 was more frequent in HCC with well to moderate differentiation compared with poorly differentiated HCC, although the difference was not statistically significant [6]. Here, we showed that the level of LGR5 expression in HCC cells affected the morphology of the tumors and their metastatic properties. Our present findings showed similar analogies with the features of clinical HCC regarding LGR5 expression. There is a possibility that high levels of LGR5 expression in HCC be the cause of the typical morphological and biological characteristics of some subclasses of HCC.

We observed similar morphological changes from various kinds of tumor cells by overexpression or down-regulation of LGR5 (unpublished data). One recent report showed that suppression of LGR5 expression in colorectal cancer cells enhanced tumor formation with increased cell motility, while cells overexpressing LGR5 tend to grow in 'colonies' with tight cell-to-cells contact and had reduction in cell motility [10]. Their observations on morphological changes and some other biological functions of LGR5 are mostly in agreement with our results, although the background of cell linage is different. Therefore, we think that our observations from the present study are not specific only to HCC, but are more generally applicable to the certain types of tumors.

Since the ligand of LGR5 has long been unknown, LGR5 has been categorized as an orphan receptor. Recently, R-spondins (Roof plate-specific Spondin, RSPOs) has been reported as ligands of LGR5 and required for sufficient activation of Wnt/β-catenin signaling [11,12,14]. To know whether overexpression of LGR5 affects the expression of RSPOs and potentiate Wnt/β-catenin signaling, we additionally measured expression of R-Spondin 1 (RSPO1) mRNA, and analyzed Wnt/β-catenin signaling level with

TOPflash/FOPflash TCF-luciferase reporter system (Supplementary Fig. 3). The expression of RSPO1 was not dependent on or related to in parallel with LGR5 expression. In HCC cell lines with high levels of LGR5 expression (HepG2), a high expression level of RSPO1 was observed. However, RSPO1 was also highly expressed in KIM 1 with low levels of LGR5. Also in LGR5-overexpressing cell (KY-G1, KY-S1) and empty vector cell (KY-V2, KY-V3), the expression of RSPO1 was not affected. In colorectal cell lines, expression level of RSPO1 was low in high LGR5 expressed cells, LoVo, whereas it was high in low expressed LGR5 cells, HCT116. We found that TOPFLASH/FOPFLASH ratio in LGR5-overexpressing KY-G1 cells was not significantly different from the vector-transfected clone. Furthermore, nuclear accumulation of β-catenin which is usually accompanied with activated Wnt signaling pathway was not detected in the LGR5-overexpressing clone (Fig. 1H). These results suggest that morphological changes and some other properties given from aberrant expression of LGR5 in tumor cells are not likely regulated by augmented Wnt signaling through R-spondin/LGR5 signaling pathway.

In this study we have shown that high levels of LGR5 expression confer cells with some of the properties of stem cells, including sphere formation and enhanced survival. In addition, high levels of LGR5 expression in vivo transformed tumors from a diffuse to a more nodular phenotype and from a metastatic to a less metastatic phenotype. These rather complicated biological roles of LGR5 may explain some of the complexity of human cancers, and further detailed studies of LGR5 would shed light on its biological functions and on the development of effective treatment strategies for cancer.

## Disclosure statement

The authors have no conflict of interest.

## Acknowledgments

We thank H. Suzuki, Y. Hashimoto and H. Abe for their excellent technical assistance. This work was supported by a Grant-in-Aid for Scientific Research (B) from the Ministry of Education, Culture, Sports, Science and Technology of Japan; and Third Term Comprehensive 10-Years Strategy for Cancer Control from the Ministry of Health, Labor and Welfare of Japan to M.S.

## Appendix A. Supporting information

Supplementary data associated with this article can be found in the online version at http://dx.doi.org/10.1016/j.yexcr.2012.10.011.

## REFERENCES

[1] H. Morita, S. Mazerbourg, D.M. Bouley, C.W. Luo, K. Kawamura, Y. Kuwabara, H. Baribault, H. Tian, A.J. Hsueh, Neonatal lethality of LGR5 null mice is associated with ankyloglossia and gastrointestinal distension, Mol. Cell. Biol. 24 (2004) 9736–9743.

[2] M.I. Garcia, M. Ghiani, A. Lefort, F. Libert, S. Strollo, G. Vassart, LGR5 deficiency deregulates Wnt signaling and leads to precocious Paneth cell differentiation in the fetal intestine, Dev. Biol. 331 (2009) 58–67.

[3] N. Barker, J.H. van Es, J. Kuipers, P. Kujala, M. van den Born, M. Cozijnsen, A. Haegebarth, J. Korving, H. Begthel, P.J. Peters, H. Clevers, Identification of stem cells in small intestine and colon by marker gene Lgr5, Nature 449 (2007) 1003–1007.

[4] N. Barker, R.A. Ridgway, J.H. van Es, M. van de Wetering, H. Begthel, M. van den Born, E. Danenberg, A.R. Clarke, O.J. Sansom, H. Clevers, Crypt stem cells as the cells-of-origin of intestinal cancer, Nature 457 (2009) 608–611.

[5] V. Jaks, N. Barker, M. Kasper, J.H. van Es, H.J. Snippert, H. Clevers, R. Toftgard, Lgr5 marks cycling, yet long-lived, hair follicle stem cells, Nat. Genet. 40 (2008) 1291–1299.

[6] Y. Yamamoto, M. Sakamoto, G. Fujii, H. Tsuiji, K. Kenetaka, M. Asaka, S. Hirohashi, Overexpression of orphan G-protein-coupled receptor, Gpr49, in human hepatocellular carcinomas with beta-catenin mutations, Hepatology 37 (2003) 528–533.

[7] K. Tanese, M. Fukuma, T. Yamada, T. Mori, T. Yoshikawa, W. Watanabe, A. Ishiko, M. Amagai, T. Nishikawa, M. Sakamoto, G-protein-coupled receptor GPR49 is up-regulated in basal cell carcinoma and promotes cell proliferation and tumor formation, Am. J. Pathol. 173 (2008) 835–843.

[8] T. McClanahan, S. Koseoglu, K. Smith, J. Grein, E. Gustafson, S. Black, P. Kirschmeier, A.A. Samatar, Identification of overexpression of orphan G protein-coupled receptor GPR49 in human colon and ovarian primary tumors, Cancer Biol. Ther. 5 (2006) 419–426.

[9] H. Uchida, K. Yamazaki, M. Fukuma, T. Yamada, T. Hayashida, H. Hasegawa, M. Kitajima, Y. Kitagawa, M. Sakamoto, Overexpression of leucine-rich repeat-containing G protein-coupled receptor 5 in colorectal cancer. Cancer Science 101 (2010) 1731–1737.

[10] F. Walker, H.H. Zhang, A. Odorizzi, A.W. Burgess, LGR5 is a negative regulator of tumourigenicity, antagonizes Wnt signalling and regulates cell adhesion in colorectal cancer cell lines. PloS one 6 (2011) e22733.

[11] W. de Lau, N. Barker, T.Y. Low, B.K. Koo, V.S. Li, H. Teunissen, P. Kujala, A. Haegebarth, P.J. Peters, M. van de Wetering, D.E. Stange, J.E. van Es, D. Guardavaccaro, R.B. Schasfoort, Y. Mohri, K. Nishimori, S. Mohammed, A.J. Heck, H. Clevers, Lgr5 homologues associate with Wnt receptors and mediate R-spondin signalling. Nature 476 (2011) 293–297.

[12] K.S. Carmon, Q. Lin, X. Gong, A. Thomas, Q. Liu, LGR5 interacts and cointernalizes with Wnt receptors to modulate Wnt/beta-catenin signaling. Molecular and Cellular Biology 32 (2012) 2054–2064.

[13] Y. Komiya, R. Habas, Wnt signal transduction pathways, Organogenesis 4 (2008) 68–75.

[14] A. Glinka, C. Dolde, N. Kirsch, Y.L. Huang, O. Kazanskaya, D. Ingelfinger, M. Boutros, C.M. Cruciat, C. Niehrs, LGR4 and LGR5 are R-spondin receptors mediating Wnt/beta-catenin and Wnt/PCP signalling. EMBO Reports 12 (2011) 1055–1061.

[15] T. Reya, S.J. Morrison, M.F. Clarke, I.L. Weissman, Stem cells, cancer, and cancer stem cells, Nature 414 (2001) 105–111.

[16] R. Pardal, M.F. Clarke, S.J. Morrison, Applying the principles of stem-cell biology to cancer, Nature Rev. 3 (2003) 895–902.

[17] N. Sato, L. Meijer, L. Skaltsounis, P. Greengard, A.H. Brivanlou, Maintenance of pluripotency in human and mouse embryonic stem cells through activation of Wnt signaling by a pharmacological GSK-3-specific inhibitor, Nature Med. 10 (2004) 55–63.

[18] X. Gong, K.S. Carmon, Q. Lin, A. Thomas, J. Yi, Q. Liu, LGR6 is a high affinity receptor of R-spondins and potentially functions as a tumor suppressor. PloS one 7 (2012) e37137.

[19] Y. Mimori-Kiyosue, C. Matsui, H. Sasaki, S. Tsukita, Adenomatous polyposis coli (APC) protein regulates epithelial cell migration and morphogenesis via PDZ domain-based interactions with plasma membranes, Genes Cells 12 (2007) 219–233.

[20] M. Chuma, M. Sakamoto, J. Yasuda, G. Fujii, K. Nakanishi, A. Tsuchiya, T. Ohta, M. Asaka, S. Hirohashi, Overexpression of cortactin is involved in motility and metastasis of hepatocellular carcinoma, J. hepatology 41 (2004) 629–636.

Liver INTERNATIONAL
OFFICIAL JOURNAL OF THE INTERNATIONAL ASSOCIATION FOR THE STUDY OF THE LIVER

Liver International ISSN 1478-3223

CLINICAL STUDIES

# Hepatic aflatoxin B1-DNA adducts and *TP53* mutations in patients with hepatocellular carcinoma despite low exposure to aflatoxin B1 in southern Japan

Ken Shirabe[1], Takeo Toshima[1], Akinobu Taketomi[1], Kennichi Taguchi[2], Tomoharu Yoshizumi[1], Hideaki Uchiyama[1], Norifumi Harimoto[3], Kiyoshi Kajiyama[3], Akinori Egashira[1] and Yoshihiko Maehara[1]

1 Department of Surgery and Science, Graduate School of Medical Sciences, Kyushu University, Fukuoka, Japan
2 Institute of Clinical Research, National Kyushu Cancer Center, Fukuoka, Japan
3 Department of Surgery, Aso Iizuka Hospital, Iizuka, Japan

**Keywords**
aflatoxin B1 – hepatitis B/C virus – hepatocellular carcinoma – *TP53*

**Abbreviations**
AFB1, aflatoxin B1; HBV, hepatitis B virus; HCC, hepatocellular carcinoma; HCV, hepatitis C virus; NBNC, non-B non-C.

**Correspondence**
Ken Shirabe, Department of Surgery and Science, Graduate School of Medical Sciences, Kyushu University, 3-1-1 Maidashi, Higashi-ku, Fukuoka 812-8582, Japan
Tel: +81 92 642 5466
Fax: +81 92 642 5482
e-mail: kshirabe@surg2.med.kyushu-u.ac.jp

Received 28 March 2011
Accepted 2 June 2011

DOI:10.1111/j.1478-3231.2011.02572.x

## Abstract

*Background & aims:* Hepatitis B or C virus infection is considered to be the main cause of hepatocellular carcinoma (HCC) in Japan. Aflatoxin B1 (AFB1) is a carcinogen associated with HCC in regions with high exposure. Mutations in codon 249, exon 7 are a hallmark of AFB1 exposure. Therefore, to clarify the role of AFB1 in hepatocarcinogenesis, we examined AFB1-DNA in liver tissue and sequenced *TP53* in Japanese patients with HCC. *Methods:* Hepatocyte AFB1-DNA adducts were determined immunohistochemically and direct sequencing of *TP53* was done to determine mutations in 188 of 279 patients who underwent hepatic resection for HCC. We assessed hepatitis C virus antibodies (HCV Ab) and HBSAg expression; patients without either were defined as having non-B non-C hepatocellular carcinoma (NBNC HCC). *Results:* AFB1-DNA adducts were detected in hepatocyte nuclei in 18/279 patients (6%), including13/83 patients (16%) with NBNC HCC and 5/51 patients (10%) expressing hepatitis B surface antigen. None of the patients with HCV Ab ($n = 136$) were positive for AFB1-DNA. The incidence of the G–T transversion and mutations in exon 7 of *TP53* in patients with AFB1-DNA adducts were significantly higher in patients with than in patients without AFB1-DNA adducts. All three patients with the codon 249 AGG–AGT mutation had AFB1-DNA adducts. *Conclusion:* Although exposure to AFB1 is thought to be low in Japan, it is still associated with hepatocarcinogenesis, particularly in NBNC HCC and hepatitis B individuals.

Hepatocellular carcinoma (HCC) is one of the most common malignant tumours worldwide. The incidence of HCC is increasing, not only in Asia, but also in western countries. However, there is a marked geographical variation in the incidence of HCC, with incidence rates ranging from 1/100 000 in parts of Northern Europe to over 1/1000 in parts of China and Southern Africa (1). This variation has been attributed to geographical differences in the prevalence of the various aetiological factors, particularly infection with chronic viral hepatitis type B and C, and aflatoxin exposure (1).

In Japan, 70–80% of HCC patients are positive for anti-hepatitis C virus (HCV) antibodies (HCV Ab) and 10–20% are positive for HBsAg (2, 3), while exposure to aflatoxin is thought to be negligible. Aflatoxins are mycotoxins produced by *Aspergillus flavus* fungi, which live in hot and humidified conditions (4). Therefore, while *A. flavus* fungi can live in tropical regions, they cannot survive in Japan. Furthermore, the Ministry of Agriculture, Forestry, and Fisheries in Japan has developed analytical methods to detect mycotoxins and assess mycotoxin contamination in food and restrict importation of food contaminated with aflatoxin B1 (AFB1) (5). Another reason why aflatoxin is rarely associated with HCC carcinogenesis in Japan is the rarity of point mutation of *TP53* at codon 249, exon 7, a mutation that has been reported as a hallmark of aflatoxin exposure (6–10).

Unfortunately, it has transpired that, despite the efforts of the Ministry of Agriculture, Forestry, and Fisheries, many people may have been exposed to aflatoxin present in food. Indeed, in 2008, it was discovered that, since 1993, rice imported from countries with high exposure to AFB1, had been illegally sold for use in food, despite only being permitted for industrial usage. Furthermore, the self-production rate of food products in Japan is 38% while the remaining 62% of foods, including nuts, cacao, spices, corn, rice, cottonseed, dry fruits and copra, which are frequently contaminated with AFB1, are imported from other countries. Based on this

situation, the risk of AFB1 contamination in Japan may not be as low as initially thought (11, 12).

The aetiology of HCC in the absence of HCV or hepatitis B virus (HBV) infection [i.e. non-B non-C (NBNC)] was reported to be <10% in Japan (13, 14). However, the incidence of patients with NBNC HCC has been reported to be increasing and the cause of this increase remains unclear (15).

Therefore, the aim of this study was to determine the association between aflatoxin and HCC in Japanese patients by determining AFB1-DNA adducts and *TP53* mutations in surgically resected HCC specimens. To our knowledge, this is the first report to show an association between aflatoxin exposure and HCC in Japan.

## Patients and methods

### Patients

Between April 2004 and December 2008, 279 patients underwent liver resection for HCC at the Department of Hepatogastroenterological Surgery at Aso Iizuka Hospital and the Department of Surgery and Science at Kyushu University Hospital in Japan. From a prospective database of these patients, these patients were included in this study. Of the patients enrolled, 91 underwent hepatectomy at Aso Iiuzka hospital and 188 at Kyushu University hospital.

The clinicopathological characteristics of the patients are as follows. There were 208 males and 71 females with a mean age of 66 years (range 17–91 years old). Among these patients, 136 (49%) patients had HCV Ab, 50 (18%) had HBsAg antibodies and nine (3%) had HCV Ab and HBsAg. The remaining 84 (30%) patients had neither HCV Ab nor HBsAg and were classified as NBNC. Patients were questioned about their drinking habits over the previous 10 years. Heavy alcohol consumption was defined as >60 g of alcohol consumed per day.

Among 84 NBNC patients, the aetiology of HCC was considered to be because of alcohol in seven patients, nonalcoholic steatohepatitis in five patients, primary biliary cirrhosis in one patient, autoimmune hepatitis in one patient, and hepatitis B core antibody (HBc Ab) positive in 31 patients. The aetiology of the remaining 34 patients was unclear.

### Detection of aflatoxin B1-DNA adducts in the resected hepatocellular carcinoma specimens by immunohistochemistry

Immunohistochemistry was performed as previously described (16, 17). Briefly, 3-μm-thick paraffin sections were dewaxed in xylene and rehydrated through a descending alcohol gradient. The sections were then washed in 0.5 M glycine in phosphate-buffered saline (PBS; pH 7.2) to inhibit/remove fixing agents, which can cause nonspecific binding of immunoperoxidase or reduce 3′,3′-diaminobenzidine tetrahydrochloride (DAB) levels. Endogenous peroxidase activity was blocked by incubating the sections in 0.3–0.5% $H_2O_2$ in absolute methanol for 30 min. The slides were then washed in Tris buffer for 5 min and incubated with few drops of 3% normal goat serum for 20–30 min. The sections were incubated overnight at 4 °C with the primary antibody against AFB1 [monoclonal anti-aflatoxin B1 (6A10); Novus Biolocals Inc., Littleton, CO, USA] diluted 1:50 in 1% bovine serum albumin in PBS. After the sections were washed three times with PBS, they were incubated with a biotin-conjugated secondary antibody for 30 min, followed by peroxidase-conjugated streptavidin for 30 min. Peroxidase activity was detected with DAB in PBS for 5 min followed by counterstaining with Mayer's haematoxylin, and dehydrated in alcohol, cleared in xylene and mounted with malinol.

Sections immunostained for AFB1 were evaluated using the labelling index by a single pathologist (K. T.) who was blinded to the patients' status. At least 1000 nuclei were counted at random in noncancerous hepatocytes from at least two sections at a magnification of ×400. Sections in which ≥5% of the hepatic nuclei expressed AFB1 were considered to be AFB1 positive.

### *TP53* mutational analysis

#### *DNA preparation*

DNA was extracted as previously described. Briefly, the frozen samples were incubated in a lysis buffer (0.01 M Tris-HCl, pH 8.0, 0.1 M EDTA, pH 8.0, 0.5% SDS) containing proteinase K (100 μg/ml) at 37 °C for 2 h. The samples were extracted twice in phenol, then in phenol/chloroform and chloroform. Following ethanol precipitation, the samples were diluted in Tris HCl and EDTA buffer (0.01 M Tris-HCl, pH 8.0, 0.01 M EDTA, pH 8.0).

#### *PCR direct sequencing of the TP53 gene*

The 275 bp fragment containing exon 6, the 439 bp fragment containing exon 7 and the 445 bp fragment containing exons 8 and 9 of the *TP53* gene were amplified by PCR (Nippon Gene Co. Ltd., Tokyo, Japan). The PCR primers for the amplification of the 406 bp fragment containing exon 5 of the *TP53* gene were: exon 5: forward, TGC AGG AGG TGC TTA CAC ATG and reverse, TCC ACT CGG ATA AGA TGC TG. Mutations of the *TP53* gene were detected by PCR direct sequencing of all PCR products using the forward and reverse primers with the dideoxynucleotide chain termination method (Bigdye sequencing kit; Applied Biosystems, Norwalk, CT, USA) followed by sequenced using an ABI Prism 310 Genetic Analyzer (Applied Biosystems).

### Statistical methods

We analysed the associations between the continuous and categorical clinicopathological variables with AFB1 adducts and *TP53* mutations using Student's *t*-tests and

$\chi^2$-tests respectively. Values of $P < 0.05$ were considered statistically significant.

## Results

### Detection of aflatoxin B1-DNA adducts

A typical section stained immunohistochemically to detect AFB1-DNA adducts is shown in Figure 1. AFB1-DNA was detected in the nuclei of hepatocytes. The median positive rate of 1000 nuclei was 31% (range, 5–80%). AFB1-DNA adducts were detected in 18/279 patients (6%). The viral infection status and rates of AFB1-DNA adduct positivity are summarized in Figure 2. AFB1-DNA adducts were detected in five patients (10%) with HBsAg and in 13 NBNC patients (16%). No AFB1-DNA adducts were detected in 135 HCV-positive patients or in nine patients positive for both HCV Ab and HBsAg. The difference in the incidence of AFB1-DNA adducts between patients with HBsAg and those with HCV Ab was statistically significant ($P < 0.0001$), as was the difference between the NBNC patients and those with HCV Ab ($P < 0.0001$).

The clinicopathological characteristics of NBNC patients with and without AFB1-DNA adducts are compared in Table 1. Overall, there were no significant differences between the two groups for any of the characteristics. None of the patients with a suspected aetiology of hepatocarcinogenesis, including alcoholism, primary biliary cirrhosis, autoimmune hepatitis and nonalcoholic steatohepatitis had evidence of AFB1-DNA adducts. The incidence of HBc Ab positivity tended to be higher among patients with AFB1-DNA adducts than among those without AFB1-DNA adducts. The extent of histological liver fibrosis tended to be milder in patients with ABF1-DNA adducts than in patients without AFB1-DNA adducts ($P = 0.1078$).

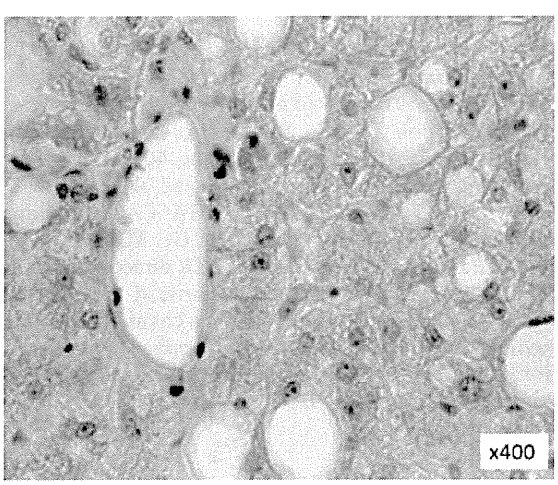


**Fig. 1.** A typical liver section stained immunohistochemically for AFB1-DNA. The AFB1-DNA adducts were detected in the nuclei of hepatocytes (original magnification, × 400).

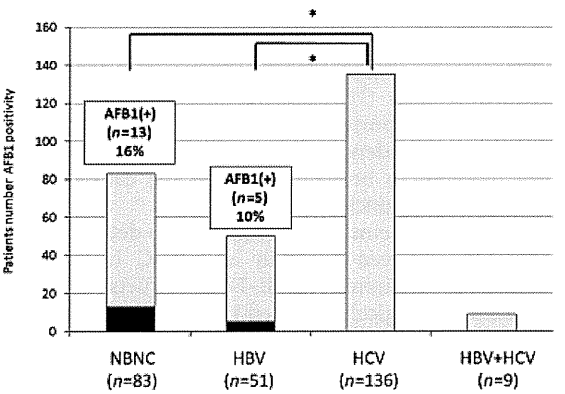


**Fig. 2.** Viral infection status and prevalence of AFB1-DNA adduct positivity. AFB1-DNA adducts were detected in 18/279 patients (6%), including five patients (10%) with HBsAg and 13 patients (16%) with NBNC. No AFB1-DNA adducts were detected in 135 HCV-positive patients or in nine patients positive for both HCV antibodies and HBsAg. The difference in the incidence of AFB1-DNA adducts between patients with HBsAg and those with HCV Ab was statistically significant (*$P < 0.0001$), as was the difference between the NBNC patients and those with HCV Ab (*$P < 0.0001$). HCV, hepatitis C virus; NBNC, non-B non-C.

### *TP*53 mutational analysis

Among 279 patients with HCC, a *TP*53 mutation was found in 41 patients (22%). The mutation was found in exon 5 in 13 patients, in exon 6 in six patients, in exon 7 in 12 patients, in exon 8 in 10 patients and in exon 9 in two patients (Fig. 3). Of 41 *TP*53 mutations detected, a G:C–T:A transversion was the most common, being present in 19 patients. The second most common mutation was a G:C–A:T, which was found in 12 patients (Fig. 4). The association between AFB1-DNA adducts and *TP*53 mutations is shown in Table 2. The incidence of *TP*53 mutations tended to be higher in patients with AFB1-DNA adducts than in patients without AFB1-DNA adducts, although this was not statistically significant ($P = 0.178$). However, the incidence of p53 mutations in exon 7 and the G–T transversion was significantly higher in patients with AFB1-DNA adducts than in those without AFB1-DNA adducts. Of note, the G–T transversion in codon 249 of *TP53* was found in three patients and all three patients had AFB1-DNA adducts.

## Discussion

Although the risk of hepatocarcinogenesis associated with exposure to AFB1 was mainly reported in countries with high exposure to AFB1, very few studies have examined this association in regions where the exposure to AFB1 is considered to be low (4). This study showed that although the codon 249 mutation of *TP53* is very rare, its presence indicates deleterious effects of aflatoxin


Liver International (2011)

**Table 1.** Clinicopathological characteristics of non-B non-C hepatocellular carcinoma patients with and without AFB1-DNA adducts

| Characteristics | AFB1 negative ($n = 70$) | AFB1 positive ($n = 13$) | *P*-value |
|---|---|---|---|
| Median age | 72 ± 10 | 67 ± 19 | 0.1428 |
| Gender | 50:20 | 9:4 | 0.9999 |
| HBc Ab(+) | 24 (35%) | 7 (54%) | 0.3567 |
| Platelets ( × $10^4$/$mm^3$) | 22 ± 10 | 20 ± 6 | 0.5253 |
| AST (IU/L) | 60 ± 101 | 46 ± 53 | 0.6231 |
| ALT (IU/L) | 43 ± 62 | 39 ± 40 | 0.8262 |
| Total bilirubin (mg/dl) | 0.7 ± 0.3 | 0.7 ± 0.3 | 0.6265 |
| Albumin (g/dl) | 3.8 ± 0.5 | 3.9 ± 0.4 | 0.5711 |
| PT (%) | 95 ± 13 | 100 ± 12 | 0.2231 |
| Mean ICGR15 (%) | 15.5 ± 8.9 | 16.4 ± 9.0 | 0.7764 |
| Aetiology | | | 0.5452 |
| Alcohol | 7 (10%) | 0 | |
| NASH | 5 (7%) | 0 | |
| PBC | 1 (1%) | 0 | |
| AIH | 1 (1%) | 0 | |
| Others | 57 (80%) | 13 (100%) | |
| Fibrosis | | | 0.7787 |
| NL | 23 (32%) | 5 (38%) | |
| CH | 24 (34%) | 5 (38%) | |
| LF | 10 (14%) | 2 (15%) | |
| LC | 14 (20%) | 1 (8%) | |

AFB1, aflatoxin B1; AIH, autoimmune hepatitis; ALT, alanine aminotransferase; AST, aspartate aminotransferase; CH, chronic hepatitis; HBc Ab, HB core antibody; ICGR15, indocyanine green retention at 15 min; LC, liver cirrhosis; LF, liver fibrosis; NASH, nonalcoholic steatohepatitis; NL, normal liver; PBC, primary biliary cirrhosis; PT, prothrombin time.

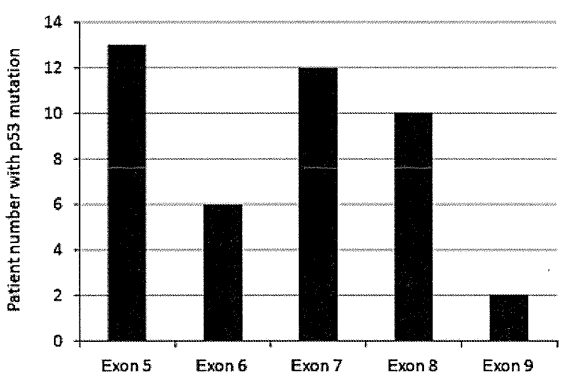


**Fig. 3.** Exon location of mutations in *TP53*. Among 279 patients with HCC, a *TP53* mutation was found in 41 patients (22%). The most common location of the mutation was exon 5, in 13 patients. Other locations included exon 6 in six patients, exon 7 in 12 patients, exon 8 in 10 patients and exon 9 in two patients.

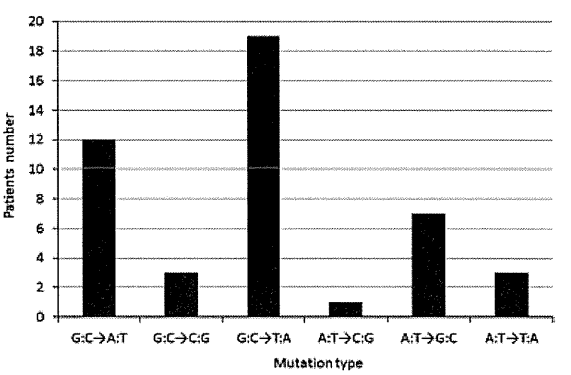


**Fig. 4.** Types of mutations detected in *TP53*. Of 41 mutations in *TP53* detected in this study, the G:C–T:A transversion was the most common (19 patients) followed by the G:C–A:T transversion (12 patients).

in HCC patients, even in countries with low exposure to AFB1. To our knowledge, no such findings in Japan have been reported until now.

The incidence of NBNC HCC is increasing in Japan. Hatanaka *et al.* (18) reported that the incidence of NBNC HCC was 5–8% in 1991–1998 and has increased to 10–12% since 1999, based on their study of 2542 Japanese patients. However, the cause of this increase remains unknown. Kusakabe *et al.* (19) reported that 18% of Japanese patients with NBNC HCC had detectable serum HBV DNA and a weak association between occult HBV infection and HCC development was observed. Therefore, this increase in NBNC HCC may be related to occult HBV infection.

In this study, AFB1-DNA adducts were detected in 18 patients and hepatitis viral infection status in these patients was unclear as none of these patients with AFB1-DNA adducts had HCV Ab, while only five patients had HBsAg. Therefore, the remaining 13 patients with AFB1-DNA adducts had neither HCV Ab nor HBsAg. However, seven of these 13 patients had HBc Ab, which suggest that they had a past history of HBV infection.

**Table 2.** *TP*53 mutations identified in non-B non-C hepatocellular carcinoma patients with and without AFB1-DNA adducts

| | AFB1-DNA adducts | | |
|---|---|---|---|
| Variables | Negative ($n = 175$) | Positive ($n = 13$) | *P*-value |
| *TP*53 mutation (+) | 38 (22%) | 5 (38%) | 0.178 |
| G–T transversion (+) | 9 (5%) | 4 (31%) | 0.0071 |
| Mutation in exon 7 (+) | 6 (3%) | 4 (31%) | 0.0023 |
| Mutation in codon 249 (+) | 0 | 3 (23%) | |

**Table 3.** Comparison of the incidence of *TP*53 mutations between countries with different levels of risk of aflatoxin B1 exposure (yes you can)

| Countries | *TP*53 mutation (%) | Exon 7 (%) | Codon 249 (G to T) (%) |
|---|---|---|---|
| Italy ($n = 90$) (32) | 26 | 6 | 1 |
| France ($n = 81$) (32) | 19 | 5 | 1 |
| China ($n = 52$) (32) | 48 | 23 | 21 |
| Japan | | | |
| With AFB1-DNA adducts ($n = 175$) | 22 | 5 | 0 |
| Without AFB1-DNA adducts ($n = 13$) | 38 | 31 | 23 |

The incidences of the p53 mutation, exon 7 and codon 249 were higher in China than in Italy and France. The incidences of these mutations in patients without AFB1-DNA adducts in our study were similar to those in Italy and France. On the other hand, the incidences of these mutations in patients with AFB1-DNA adducts in this study were similar to those reported in China.
AFB1, aflatoxin B1.

Accordingly, hepatitis B infection was associated with AFB1-DNA adducts in 12/18 patients.

AFB1 has been reported to considerably increase the risk of HCC in patients with HBV infection. The incidence of the relative risk of HCC in patients with HBV infection were 4.8–17.4 times that of patients without AFB1 exposure, while the relative risk of HCC in patients exposed to AFB1 but without HBV was 1.9–17.4. Notably, the relative risk increased to 59.4–70.0 among patients with both HBV infection and AFB1 exposure (20–23). These findings indicate that exposure to AFB1 strongly enhances the hepatocarcinogenesis of HBV infection. Nevertheless, almost no data are available on the influence of aflatoxin in low exposure regions. In this series, because the incidence of AFB1-DNA adducts in patients with HBsAg and NBNC patients with HBc Ab was significantly higher than that in the patients with HCV Ab, exposure to AFB1 may enhance hepatocarcinogenesis of HBV infection in Japan.

The *TP*53 mutation of codon 249, which is a common feature associated with exposure to AFB1 (24–26) has not yet been reported in Japan (27–30). The G–T transversion and exon 7 mutation of *TP*53 have also been reported to be related to AFB1 exposure (27, 31). In this study, three patients had this mutation, all of whom had AFB1-DNA adducts. The incidence of these mutations was significantly higher in patients with AFB1-DNA adducts than in the patients without AFB1-DNA adducts. Pineau *et al.* (32) compared the *TP*53 status in patients with HCC in China where the intake of AFB1 is high and in patients in European countries, such as Italy and France, where the intake of AFB1 is low. Therefore, we compared the incidence of *TP*53 between countries with different levels of risk of AFB1 exposure, including our own results (Table 3). The incidence of the p53 mutation in China was 48%, which was significantly higher than that in Italy and France, where the incidence was 26 and 19% respectively. The rates of mutation in exon 7 and codon 249 were 6 and 1% in Italy, 5 and 1% in France and 23 and 21% in China, which was also statistically significant. The incidences of mutations in *TP*53, exon 7 and codon 249 in our study were 23, 7 and 2% respectively. These data were quite similar to those in Italy and France and previously reported from Japan (7, 28–30). Nevertheless, the incidence of *TP*53 mutations in patients with AFB1-DNA adducts was much higher than in those without AFB1-DNA adducts. The incidence of *TP*53 mutation in patients with AFB1-DNA adducts was 38%, that of mutations in exon 7 was 31% and that of p53 mutations of codon 249 was 23%, which were quite similar to those reported in China. These data also suggest that AFB1 promotes hepatocarcinogenesis in Japan.

The possible mechanism by which AFB1 causes DNA mutation remains unclear. Smela *et al.* (33) noted that the primary DNA adduct of AFB1 is 8,9-dihydro-8-($N^7$-guanyl)-9-hydroxyaflatoxin B1 (AFB1-N7-Gua), which is normally converted to two secondary products, an apurinic site and an AFB1-formamidopyrimine (AFB1-FAPY) adduct. AFB1-FAPY was found to cause a G to T mutation in *Escherichia coli*. AFB1-FAPY also blocks replication, even when the efficient bypass polymerase MucAB is used by the cell. Smela and colleagues concluded that AFB1-FAPY may be the primary candidate for the genotoxicity and mutagenicity associated with AFB1 that may ultimately lead to liver cancer. AFB1 metabolites can also bind to guanine at other codons of *TP53*, notably 245, 248 and 273, which are mutation

'hot spots' in many cancers, but not in HCC associated with AFB1. To examine this site-specific mutagenesis, Besaratinia *et al.* (31) exposed cII transgenic mouse fibroblasts to AFB1 *in vitro* and detected G to T transversions in codons 42 and 45 of the cII transgene, which have identical sequence contexts to those of codon 249 of human *TP*53. These codons include two frequently mutated sites in AFB1-exposed cells that contain the G to T transversion signature mutation at their third base positions.

Tumour-derived p53 mutant proteins contribute to carcinogenesis though three overlapping mechanisms: loss of function, dominant-negative effects and gain-of-function effects. Gouas *et al.* (34) demonstrated that p.R249S (a mutation at codon 249 of AGG to AGT, arginine to serine) has lost the capacity to bind to p53 response elements and to transactivate the p53 target genes in HCC cell lines. p.R249S itself did not show gain-of-function effects, but it did interact with the HBV X gene, conferring a subtle growth advantage early in the transformation process. Therefore, further examination of hepatitis B virus X protein may be helpful to better understand the carcinogenesis of NBNC HCC. Indeed, occult HBV infection has been reported to be one of the carcinogenic mechanisms in Japanese patients with NBNC HCC. On the other hand, carcinogenesis involving AFB1 and *TP53* has not been reported for other human organs. AFB1 is metabolized in the liver by cytochrome P450 to generate covalent, promutagenic DNA adducts. The interaction between the AFB1-DNA adduct and HBV X protein may explain the liver-specific carcinogenic effects of AFB1, because hepatitis B infection seems to be liver specific.

In conclusion, the effects of AFB1 are not negligible in hepatocarcinogenesis, even in Japan. This may be important in patients with HBV and in patients with NBNC HCC, but not in HCV HCC patients. The *TP*53 mutations in HCC may be related to AFB1 exposure. Further epidemiological studies are necessary to better understand the role of AFB1 exposure in hepatocarcinogenesis in Japan.

## Acknowledgements

*Conflict of interest*: None of the authors have any association that poses a possible conflict of interest in connection with the manuscript.
*Financial support*: None.

## References

1. Montalto G, Cervello M, Giannitrapani L, *et al.* Epidemiology, risk factors, and natural history of hepatocellular carcinoma. *Ann NY Acad Sci* 2002; **963**: 13–20.
2. Shiratori Y, Shiina S, Imamura M, *et al.* Characteristic difference of hepatocellular carcinoma between hepatitis B- and C-viral infection in Japan. *Hepatology* 1995; **22**: 1027–33.
3. Nishioka K, Watanabe J, Furuta S, *et al.* A high prevalence of antibody to the hepatitis C virus in patients with hepatocellular carcinoma in Japan. *Cancer* 1991; **67**: 429–33.
4. Ozdemir FT, Tiftikci A, Sancak S, *et al.* The prevalence of the mutation in codon 249 of the P53 gene in patients with hepatocellular carcinoma (HCC) in Turkey. *J Gastrointest Cancer* 2010; **41**: 185–9.
5. Tanaka K, Sago Y, Zheng Y, Nakagawa H, Kushiro M. Mycotoxins in rice. *Int J Food Microbiol* 2007; **119**: 59–66.
6. Nose H, Imazeki F, Omata M. p53 gene mutations and 17p allelic deletions in hepatocellular carcinoma from Japan. *Cancer* 1993; **72**: 355–60.
7. Hayashi H, Sugio K, Matsumata T, *et al.* The clinical significance of p53 gene mutation in hepatocellular carcinoma in Japan. *Hepatology* 1995; **22**: 1702–7.
8. Okada T, Iizuka N, Yamada-Okabe H, *et al.* Gene expression profile linked to p53 status in hepatitis C virus-related hepatocellular carcinoma. *FEBS Lett* 2003; **555**: 583–90.
9. Ding X, Park YN, Taltavull TC, *et al.* Geographic characterization of hepatitis virus infections, genotyping of hepatitis B virus, and p53 mutation in hepatocellular carcinoma analyzed by in situ detection of viral genomes from carcinoma tissues: comparison among six different countries. *Jpn J Infect Dis* 2003; **56**: 12–8.
10. Wong N, Lai P, Pang E, *et al.* Genomic aberrations in human hepatocellular carcinomas of different etiologies. *Clin Cancer Res* 2000; **6**: 4000–9.
11. Sugita-Konoshi Y, Nakajima M, Tabata S, *et al.* Occurrence of aflatoxins, ochratoxin A, and fumonisins in retail foods in Japan. *J Food Prot* 2006; **69**: 1365–70.
12. Kumagai S, Nakajima M, Tabata S, *et al.* Aflatoxin and ochratoxin A contamination of retail foods and intake of these mycotoxins in Japan. *Food Addit Contam* 2008; **25**: 1101–6.
13. Tomimaru Y, Sasaki Y, Yamada T, *et al.* Fibrosis in noncancerous tissue is the unique prognostic factor for primary hepatocellular carcinoma without hepatitis B or C viral infection. *World J Surg* 2006; **30**: 1729–35.
14. Watabe H, Shiratori Y, Tateishi R, *et al.* Clinical features of patients with HCC who are negative for both HBV and HCV markers. *Hepatogastroenterology* 2003; **50**: 2157–60.
15. Abe H, Yoshizawa K, Kitahara T, *et al.* Etiology of non-B non-C hepatocellular carcinoma in the eastern district of Tokyo. *J Gastroenterol* 2008; **43**: 967–74.
16. Chen CJ, Zhang YJ, Lu SN, Santella RM. Aflatoxin B1 DNA adducts in smeared tumor tissue from patients with hepatocellular carcinoma. *Hepatology* 1992; **16**: 1150–5.
17. Murugavel KG, Naranatt PP, Shankar EM, *et al.* Prevalence of aflatoxin B1 in liver biopsies of proven hepatocellular carcinoma in India determined by an in-house immunoperoxidase test. *J Med Microbiol* 2007; **56**: 1455–9.
18. Hatanaka K, Kudo M, Fukunaga T, *et al.* Clinical characteristics of NonBNonC-HCC: comparison with HBV and HCV related HCC. *Intervirology* 2007; **50**: 24–31.

19. Kusakabe A, Tanaka Y, Orito E, *et al.* A weak association between occult HBV infection and non-B non-C hepatocellular carcinoma in Japan. *J Gastroenterol* 2007; **42**: 298–305.
20. Qian GS, Ross RK, Yu MC, *et al.* A follow-up study of urinary markers of aflatoxin exposure and liver cancer risk in Shanghai, People's Republic of China. *Cancer Epidemiol Biomarkers Prev* 1994; **3**: 3–10.
21. Ross RK, Yuan JM, Yu MC, *et al.* Urinary Aflatoxin biomarkers and the risk of hepatocellular carcinoma. *Lancet* 1992; **339**: 943–6.
22. Wang LY, Hatch M, Chen CJ, *et al.* Aflatoxin exposure and risk of hepatocellular carcinoma in Taiwan. *Br J Cancer* 1996; **67**: 620–30.
23. Lunn R M, Zhang YJ, Wang LY, *et al.* Mutations, chronic hepatitis B virus infection, and aflatoxin exposure in hepatocellular carcinoma in Taiwan. *Cancer Res* 1997; **57**: 3471–7.
24. Ozturk M. p53 mutation in hepatocellular carcinoma after aflatoxin exposure. *Lancet* 1991; **338**: 1356–9.
25. Montesano R, Hainaut P, Wild CP. Hepatocellular carcinoma: from gene to public health. *J Natl Cancer Inst* 1997; **89**: 1844–51.
26. Ming L, Thorgeirsson SS, Gail MH, *et al.* Dominant role of hepatitis B virus and cofactor role of aflatoxin in hepatocarcinogenesis in Qidong, China. *Hepatology* 2002; **36**: 1214–20.
27. Stern MC, Umbach DM, Yu MC, *et al.* Hepatitis B, aflatoxin B1, and p53 codon 249 mutation in hepatocellular carcinomas from Guangxi, People's Republic of China and a meta-analysis of existing studies. *Cancer Epidemiol Biomarkers Prev* 2001; **10**: 617–25.
28. Konishi M, Kikuchi-Yanoshita R, Tanaka K, *et al.* Genetic changes and histopathological grades in human hepatocellular carcinoma. *Jpn J Cancer Res* 1993; **84**: 893–9.
29. Nishida N, Fukuda Y, Kokuryu H, *et al.* Role and mutational heterogeneity of the p53 gene in hepatocellular carcinoma. *Cancer Res* 1993; **53**: 368–72.
30. Oda T, Tsuda H, Scarpa A, Sakamoto M, Hirohashi S. p53 gene mutation spectrum in hepatocellular carcinoma. *Cancer Res* 1994; **1992**: 6358–64.
31. Besaratinia A, Kim S, Hainaut P, Pfeifer GP. In vitro recapitulating of *TP* 53 mutagenesis in hepatocellular carcinoma associated with dietary aflatoxin B1 exposure. *Gastroenterology* 2009; **137**: 1127–37.
32. Pineau P, Marchio A, Battiston C, *et al.* Chromosome instability in human hepatocellular carcinoma depends on p53 status and aflatoxin exposure. *Mutat Res* 2008; **653**: 6–13.
33. Smela ME, Hamm ML, Henderson PT, *et al.* The aflatoxin B1 formamidopyrimidine adduct plays a major role in causing the types of mutations observed in human hepatocellular carcinoma. *PNAS* 2002; **99**: 6655–60.
34. Gouas DA, Shi H, Hautefeuille AH, *et al.* Effects of the TP53 p.R249S mutation on proliferation and clonogenic properties in human hepatocellular carcinoma cell lines: interaction with hepatitis B virus X protein. *Carcinogenesis* 2010; **31**: 1475–82.

Research Article

EASL EUROPEAN ASSOCIATION FOR THE STUDY OF THE LIVER | JOURNAL OF HEPATOLOGY

# Diacylglycerol kinase alpha enhances hepatocellular carcinoma progression by activation of Ras–Raf–MEK–ERK pathway

Kazuki Takeishi[1], Akinobu Taketomi[1,*], Ken Shirabe[1], Takeo Toshima[1], Takashi Motomura[1], Toru Ikegami[1], Tomoharu Yoshizumi[1], Fumio Sakane[2], Yoshihiko Maehara[1]

[1]*Department of Surgery and Science, Graduate School of Medical Sciences, Kyushu University, Fukuoka, Japan;* [2]*Department of Chemistry, Graduate School of Science, Chiba University, Chiba, Japan*

**Background & Aims**: Diacylglycerol kinases (DGKs) were recently recognized as key regulators in cell signaling pathways. We investigated whether DGKα is involved in human hepatocellular carcinoma (HCC) progression.

**Methods**: We silenced or overexpressed DGKα in HCC cells and assessed its effect on tumor progression. DGKα expression in 95 surgical samples was analyzed by immunohistochemistry, and the expression status of each sample was correlated with clinicopathological features.

**Results**: DGKα was detected in various HCC cell lines but at very low levels in the normal liver. Knockdown of DGKα significantly suppressed cell proliferation and invasion. Overexpression of wild type (WT) DGKα, but not its kinase-dead (KD) mutant, significantly enhanced cell proliferation. DGKα knockdown impaired MEK and ERK phosphorylation, but did not inhibit Ras activation in HCC cells. In a xenograft model, WT DGKα overexpression significantly enhanced tumor growth compared to the control, but KD DGKα mutant had no effect. Immunohistochemical studies showed that DGKα was expressed in cancerous tissue, but not in adjacent non-cancerous hepatocytes. High DGKα expression ($\geqslant$20%) was associated with high Ki67 expression ($p$ <0.05) and a high rate of HCC recurrence ($p$ = 0.033) following surgery. In multivariate analyses, high DGKα expression was an independent factor for determining HCC recurrence after surgery.

**Conclusions**: DGKα is involved in HCC progression by activation of the MAPK pathway. DGKα could be a novel target for HCC therapeutics as well as a prognostic marker.



Keywords: Liver cancer; Diacylglycerol; Phosphatidic acid; Diacylglycerol kinase; MAP kinase.

*Received 21 November 2011; received in revised form 2 February 2012; accepted 13 February 2012; available online 14 March 2012*

* Corresponding author. Address: Department of Surgery and Science, Graduate School of Medical Sciences, Kyushu University, 3-1-1, Maidashi, Higashi-ku, Fukuoka 812-8582, Japan. Tel.: +81 92 642 5466; fax: +81 92 642 5482.

*E-mail address:* taketomi@surg2.med.kyushu-u.ac.jp (A. Taketomi).

*Abbreviations:* HCC, hepatocellular carcinoma; MAPK, mitogen-activated protein kinase; DGK, diacylglycerol kinase; DG, diacylglycerol; PA, phosphatidic acid; siRNA, small interfering RNA; ERK, extracellular signal-regulated kinase; MEK, MAPK/ERK kinase; HGF, hepatocyte growth factor; WT, wild type; KD, kinase dead; FACS, fluorescence activated cell sorting.

## Introduction

Hepatocellular carcinoma (HCC) is one of the most common solid tumors worldwide and its incidence is continuing to increase [1,2]. The main therapies for HCC are curative strategies such as liver resection or liver transplantation [3,4]. As these treatments are only viable for patients with preserved liver function, or for those with access to a donor organ, there are many patients with incurable HCC [5,6]. In addition, the long-term outcome after these therapies remains unsatisfactory because of high recurrence rates [3,5]. Therefore, new novel therapeutic strategies for HCC are required.

HCC is associated with increased expression and activity of mitogen-activated protein kinase (MAPK) signaling intermediates [7,8]. Activated Ras induces the Raf–MAPK/ERK kinase (MEK)-extracellular signal-regulated kinase (ERK) cascade, which regulates various cellular responses, including proliferation, survival, and migration [7–9].

Diacylglycerol kinase (DGK) catalyzes the phosphorylation of diacylglycerol (DG) to generate phosphatidic acid (PA) [10–14]. DG and PA are recognized as important second messengers, and play key roles in signal transduction and cellular function [11–14]. DGKs have critical tasks in signal transmission from many receptors, and modulate diverse cellular processes, regulating both DG and PA levels. To date, 10 mammalian DGK isozymes (α–θ) have been identified, and all have the catalytic region in common [10–14]. DGKα is subdivided into the type I group due to its calcium-binding EF-hand motifs and recoverin homology domain [15–17]. This enzyme was first identified in T lymphocytes/thymus and enhances interleukin 2-induced T cell proliferation [15,18,19]. Another report demonstrated that DGKα overexpression resulted in a defect in T cell receptor signaling characteristic of anergy [20,21]. These reports collectively suggest that DGKα has various biological roles.

Here, we found that DGKα was expressed in several human liver cancer cell lines, but only at very low levels in the normal liver. In order to identify HCC-specific functions of DGKα, this isoform was downregulated and then conversely overexpressed in two types of HCC cell lines by transfecting small interfering RNA (siRNA) and DGKα expression plasmids, respectively. Interestingly, this study clarified that DGKα positively regulated proliferation and invasion of human HCC cells through activation of MAPK signaling. Furthermore, immunohistochemical studies

Cancer

of surgical samples suggested that high DGKα expression was associated with HCC recurrence after surgery.

## Materials and methods

*Cell culture*

Human HCC cell lines, HuH7, PLC/PRF/5, HLE, and Hep3B, were cultured in Dulbecco's modified Eagle's medium supplemented with 10% fetal bovine serum, 100 IU/ml penicillin, and 100 mg/ml streptomycin sulfate (Life Technologies, Inc., Carlsbad, CA). All cells were maintained at 37 °C in 5% $CO_2$.

*Antibodies and reagents*

Anti-pig DGKα polyclonal antibodies (cross-reactive with human DGKα) were prepared as described previously [22]. Other antibodies were obtained from commercial sources as follows: anti-Ras antibody (Upstate Biotechnology, Inc., Waltham, MA), anti-ERK1/2, anti-phosphorylated-ERK1/2 (Thr-202/Tyr-204), anti-MEK1/2, and anti-phosphorylated-MEK1/2 (Ser-217/221) antibodies (Cell Signaling Technology Inc., Beverly, MA), anti-actin, anti-GAPDH and anti-cyclin D1 monoclonal antibodies (Santa Cruz Biotechnology Inc., Santa Cruz, CA), anti-Ki67 monoclonal antibodies (Dako, Tokyo, Japan) and anti-GFP monoclonal antibodies (Nacalai Tesque, Kyoto, Japan). Recombinant human hepatocyte growth factor (HGF) was purchased from Peprotech (Rocky Hill, NJ).

*Human tissue samples*

Samples from 95 patients who had undergone liver resection for HCC without preoperative treatment at the Department of Surgery and Science, Kyushu University Hospital, between January 1998 and December 2002 were analyzed by immunohistochemistry. Patients' clinical features are shown in Table 1. Histological diagnoses of the tumors were based on the General Rules for the Clinical and Pathological Study of Primary Liver Cancer by the Liver Cancer Study Group of Japan [23]. Written, informed consent was obtained from each patient for the study of tissue excised from surgical specimens. The Kyushu University Medical human investigation committee gave approval for this study.

*Plasmids*

cDNAs encoding wild type (WT) DGKα and kinase-dead (KD) DGKα were generated as previously described [15,24] and were subcloned into pEGFP-C3 and pcDNA 1.1 vectors. Cells were transiently transfected using Lipofectamine LTX (Invitrogen, Carlsbad, CA), according to the manufacturer's instructions. To generate stable cell lines that permanently expressed exogenous GFP alone, GFP–DGKα WT or GFP–DGKα KD, 1 μg of linearized DNA was transfected, and cells were selected for neomycin resistance using 2 mg/ml of G418. Individual clones were isolated and tested for expression of GFP by Western blot analysis.

*Immunohistochemistry*

Paraffin sections of samples were deparaffinized. Heat-induced epitope retrieval was performed in 0.1 M NaOH citrate buffer (pH 7.0), and the samples were heated in an autoclave. Immunoreactivity was independently graded by two liver pathologists. At least 1000 cancer cells in five high-power fields were counted.

*RNA interference*

To silence the expression of human DGKα, the following oligonucleotides (Invitrogen, Carlsbad, CA) were used: *DGKα1* sense; 5′-CGAGGAUGGCGAGAUGGCUAAAUAU-3′, and *DGKα2* sense; 5′-GCGAGUCAAGCAUUGGUCUUGGCAA-3′. As a negative control, scrambled siRNA was used. The annealed oligonucleotide duplex siRNA (10 nM) was transfected into cells using Lipofectamine RNAi max (Invitrogen, Carlsbad, CA) according to the manufacturer's instructions.

*Cell proliferation assays*

PLC/PRF/5 and HuH7 cells were seeded in 60 mm dishes at a density of $2 \times 10^5$. After days 0, 2, 4, 6, and 8 of transfection with plasmid or siRNA, cells were trypsinized. Cells excluding trypan blue were counted using a hemocytometer.

*Invasion assays*

Invasion analyses were performed as described previously [25]. Invasive indexes were calculated using the following formula: Invasion index (%) = (number of cells that invaded through Matrigel insert membrane)/(number of cells that migrated through control insert membrane). Each experiment was performed in triplicate wells and repeated three times.

*Protein extraction and Western blot analysis*

Protein extraction and Western blot analysis were performed as described [26]. To measure the relative density of immunoreactive bands, images were scanned and analyzed by Image J software (National Institute of Health., Bethesda, MD).

*Affinity precipitation of activated Ras*

Cells were lysed in lysis buffer (50 mM Tris pH 7.5, 10 mM $MgCl_2$, 0.5 M NaCl, and 2% Igepal). The supernatant was incubated with 10 μl of Raf–Ras–binding domain (RBD)–GST beads (Cytoskeleton Inc., Denver, CO), which selectively interacted with active GTP–bound Ras. The beads were washed three times with wash buffer (25 mM Tris pH 7.5, 30 mM $MgCl_2$, 40 mM NaCl) containing 5 mM $MgCl_2$, and then boiled in SDS sample buffer. Ras associated with Raf–RBD–GST and total Ras in cell lysates were detected with anti-Ras antibody using Western blot analysis.

*Fluorescence-activated cell sorting (FACS)*

HCC cells were transfected with siRNA. After 48 h, cells were incubated with 40 ng/ml of HGF for 48 h. Adherent and floating cells were then pooled and washed with ice-cold PBS. Cells were fixed with ice-cold 70% ethanol and labeled with PI, followed by FACS. G1, S and G2/M populations were quantified using FACS Scan Cell Sorter (BD Biosciences, Tokyo, Japan) using FlowJo software (Tree Star, Ashland, OR).

*Xenograft model*

BALB/c male nude mice (Charles River, Yokohama, Japan) were maintained according to the Institutional Animal Care and Use Committee of the Kyushu University Graduate School of Medical Sciences. Tumors were generated by subcutaneously injecting $5 \times 10^6$ PLC/PRF/5 cells stably expressing endogenous GFP alone, GFP–DGKα WT, or GFP–DGKα KD. Tumor dimensions were measured once a week, and tumor volume was calculated using the following formula: tumor volume ($mm^3$) = (the largest diameters)/2 × (the smallest diameters)/2 [27]. Mice were euthanized when tumors reached 10% of their body weight or when the skin overlying tumors became ulcerated.

*Statistical analysis*

JMP 8J Version (SAS Institute, Cary, NC) was used for all analyses. All experiments were independently performed three times in triplicate. Comparisons between groups were made using Wilcoxon test with continuous variables and Fisher's exact test for comparisons of proportions. Survival curves were estimated using the Kaplan–Meier method, and the differences in survival rates between groups were compared by the log-rank test. Multivariate analysis was performed using Cox's proportional hazard regression model to evaluate the independent factors predictive of patients' survival. By multivariate analysis, we examined the following six clinicopathological factors, which were significant factors in the univariate analysis: (1) positive for hepatitis C virus antibody; (2) indocyanine green 15-min retention test (>15% *vs.* ⩽15%); (3) positive for intrahepatic metastasis; (4) DGKα (high *vs.* low expression); (5) liver cirrhosis, (6) AFP (>40 *vs.* ⩽40). Data are expressed as mean ± standard deviation. $p$ Values of <0.05 were considered to be significant.

**Table 1. Relationship between DGKα expression and clinicopathological factors.**

| Factors | All patients | DGKα expression | | *p* value |
|---|---|---|---|---|
| | | Low | High | |
| | (n = 95) | (n = 78) | (n = 17) | |
| Gender, male (%) | 80 | 78 | 88 | 0.51 |
| Age (yr) | 63 ± 9 | 64 ± 10 | 61 ± 9 | 0.41 |
| HBsAg positive (%) | 21 | 19 | 29 | 0.34 |
| Anti-HCV Ab positive (%) | 61 | 60 | 65 | 0.79 |
| Albumin (g/dl) | 4.0 ± 0.4 | 4.0 ± 0.4 | 4.0 ± 0.5 | 0.59 |
| Total bilirubin (mg/dl) | 0.9 ± 0.3 | 0.9 ± 0.3 | 0.9 ± 0.3 | 0.60 |
| AST (IU/L) | 51 ± 28 | 52 ± 29 | 45 ± 22 | 0.38 |
| ALT (IU/L) | 54 ± 43 | 53 ± 34 | 64 ± 73 | 0.34 |
| ICG-R15 (%) | 16 ± 9 | 16 ± 8 | 15 ± 8 | 0.49 |
| Platelet (x $10^3$/μl) | 69 ± 114 | 69 ± 124 | 78 ± 84 | 0.77 |
| Child-Pugh A/B, C (%) | 84/16 | 84/16 | 88/12 | 0.49 |
| AFP (ng/ml) | 7050 (1.7-41,000) | 9000 (1.7-5600) | 607 (5.3-41,000) | 1.00 |
| Cirrhosis (%) | 31 | 31 | 24 | 0.77 |
| Tumor size (cm) | 4.2 ± 3.1 | 4.2 ± 3.2 | 4.7 ± 2.6 | 0.54 |
| Stage I, II/III, IV (%)* | 42/58 | 45/55 | 24/76 | 0.17 |
| Differentiation: well, moderately/poorly (%) | 70/30 | 68/32 | 76/24 | 0.57 |
| Portal vein invasion (%) | 47 | 46 | 59 | 0.43 |
| Intrahepatic metastasis (%) | 23 | 19 | 41 | 0.06 |

DGKα, diacylglycerol kinase α; HBsAg, hepatitis B surface antigen; anti-HCV Ab, anti- hepatitis C virus antibody; ALT, alanine aminotransferase; AST, aspartate aminotransferase; ICG-R15, indocyanine green 15-min retention test; AFP, α-fetoprotein.
*Tumor staging was defined according to the Liver Cancer Study Group of Japan [23].

## Results

### *DGKα is upregulated in HCC*

DGKα expression in HCC cell lines was examined by Western blotting. Fig. 1A shows that DGKα was expressed in all HCC cell lines, but was almost insignificant in primary cultured normal hepatocytes prepared from surgically resected specimens of patients with liver metastasis, indicating that DGKα is expressed in HCC and the expression is stronger than in non-cancerous hepatocytes.

### *Knockdown of DGKα suppresses HCC cell proliferation and invasion*

To determine the role of DGKα in HCC, DGKα expression was suppressed by siRNA in two HCC cell lines, PLC/PRF/5 and HuH7. We used these cell lines for analysis because they have different features: PLC/PRF/5 cells are positive for hepatitis B surface antigen and represent poorly differentiated HCC, whereas HuH7 cells are negative for hepatitis B surface antigen and represent well differentiated HCC [28,29]. *DGKα*-specific siRNA successfully silenced the expression of DGKα 48 h after transfection in PLC/PRF/5 (Supplementary Fig. 1A) and HuH7 (data not shown) cells. As previous reports demonstrated that DGKα positively regulates T cell proliferation and vascular endothelial cell invasion [18,30], the proliferation and invasion of *DGKα*-silenced HCC cells were compared to those of wild type cells. Knockdown of DGKα expression significantly inhibited HCC cell proliferation (Fig. 1B and C). FACS analysis also showed that loss of DGKα increased G1 phase and reduced G2/S phase of HCC cells (Fig. 1D). Furthermore, DGKα knockdown decreased cyclin D1 expression, indicating that it may be a target of DGKα (Fig. 1E). Next, the invasive activity of DGKα in HCC cells was investigated. Silencing of *DGKα* reduced cell invasion (Fig. 1F). These results suggest that DGKα plays a key role in promoting HCC cell proliferation and invasion.

### *Overexpression of DGKα catalytic activity promotes HCC cell proliferation*

In the reverse experiment, we overexpressed DGKα in HCC cells. Exogenous GFP alone, GFP–DGKα WT, and GFP–DGKα KD proteins were expressed by transfecting plasmids (Supplementary Fig. 1B); exogenous WT DGKα expression was about five times that of endogenous DGKα in HCC cells (data not shown). WT DGKα overexpression significantly enhanced HCC cell proliferation (Fig. 2A and B). Although the expression level of KD DGKα was almost the same as that of WT DGKα (Supplementary Fig. 1B), this mutant failed to affect the extent of cell proliferation (Fig. 2A and B), indicating that DGKα catalytic activity is required to promote cell proliferation.

### *DGKα activates the Ras–Raf–MEK–ERK pathway in HCC cells*

To elucidate the mechanism by which DGKα enhances cell proliferation and invasion, HGF-induced ERK1/2 activation in *DGKα*-silenced HCC cells was subsequently examined. It has been reported that activation of the Ras–Raf–MEK–ERK pathway is ubiquitous in human HCC, and its activation is associated with tumor growth and invasion [8,31]. In PLC/PRF/5 and HuH7, DGKα depletion significantly inhibited the increase in ERK1/2 phos-

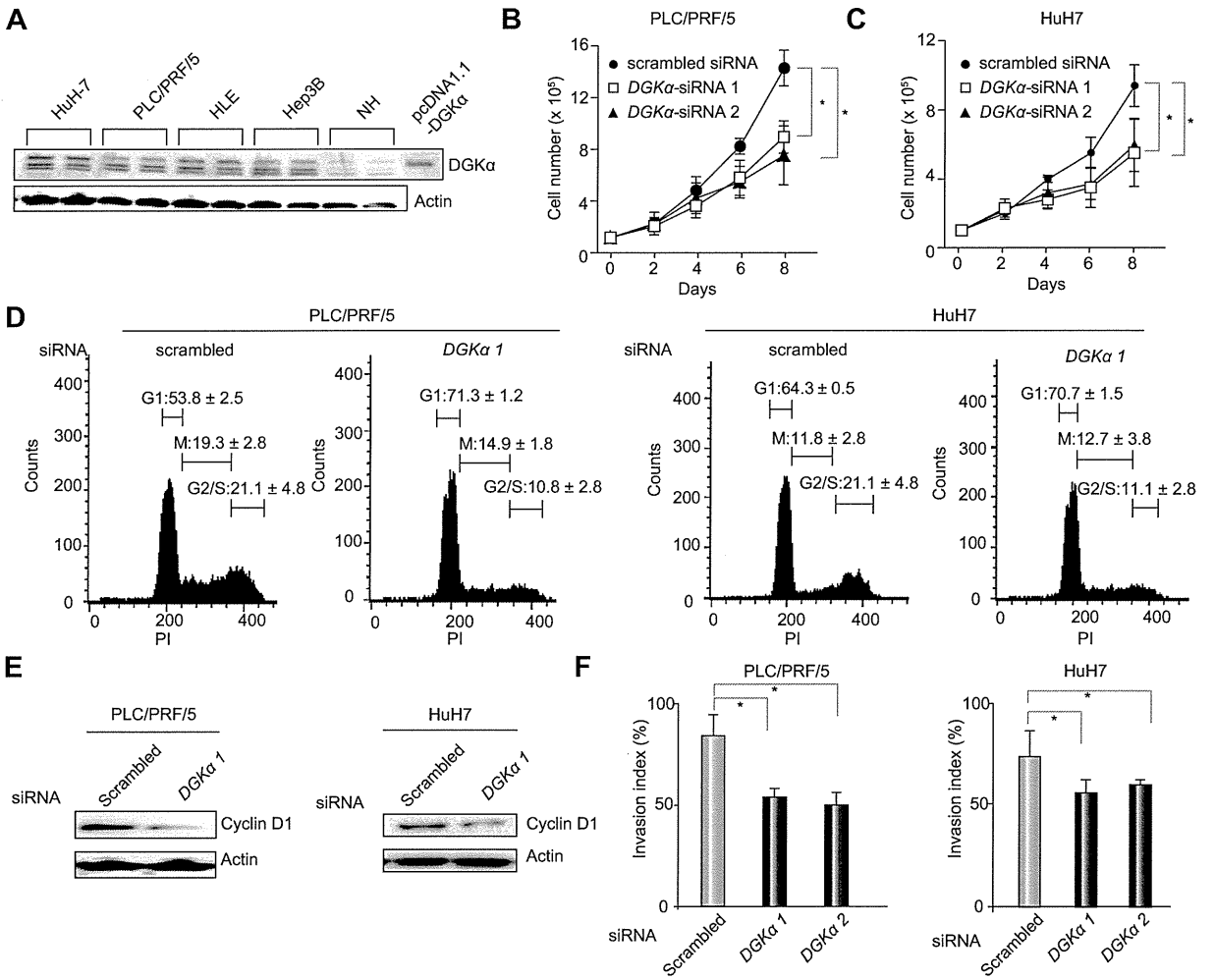


**Fig. 1. DGKα expression in HCC cell lines and inhibition of HCC cell proliferation and invasion caused by silencing of *DGKα*.** (A) DGKα expression in human HCC cells and normal hepatocytes (NH) was analyzed. At the indicated times after transfections, (B) PLC/PRF/5 and (C) HuH7 cells were counted. (D) Histograms show DNA content (*x*-axis) plotted *vs.* relative cell number (*y*-axis). (E) After DGKα knockdown, cyclin D1 expression was analyzed. (F) Following DGKα knockdown, cancer cells that had migrated through the membrane to the lower surface were counted. Data shown are representative of at least three experiments. Asterisks (*) indicate statistical significance between DGKα-specific and scrambled siRNA.

phorylation, following stimulation with HGF for 5 min, by 90% and 50%, respectively (Fig. 2C and D and Supplementary Fig. 2A and D). The effect of *DGKα* silencing on HGF-induced phosphorylation of kinases upstream of ERK1/2, MEK1/2 was subsequently examined. In PLC/PRF/5 and HuH7, depletion of DGKα also inhibited MEK1/2 phosphorylation, following 5 min of HGF stimulation, by 55% and 50%, respectively (Fig. 2C and D and Supplementary Fig. 2B and E). In contrast, DGKα depletion did not impair the activity of Ras following 5 and 30 min of HGF stimulation, but significantly activated Ras compared with the control, following HGF stimulation for 60 min in PLC/PRF/5 and HuH7, by 40% and 50%, respectively (Fig. 2C and D and Supplementary Fig. 2C and F). Collectively, these results suggest that DGKα plays an important role in activation of HGF-induced MAPK pathways, and that the target component of DGKα is upstream of MEK and downstream of Ras.

*DGKα induces tumor growth in xenograft models*

We generated stable cell lines expressing either exogenous GFP alone, GFP–DGKα WT or GFP–DGKα KD. To investigate whether DGKα enhanced tumor growth *in vivo*, xenograft models were generated by subcutaneous injection of these stable transformants. Successful overexpression in xenograft models was confirmed by Western blotting (Fig. 3C). Overexpression of WT DGKα promoted significant subcutaneous tumor growth compared to that of GFP alone (Fig. 3A). There were no significant differences in tumor growth between GFP alone and KD DGKα (Fig. 3B). Overexpression of WT DGKα, but not KD DGKα, activated MEK and ERK, and induced cyclin D1 upregulation (Fig. 3C). Ki67 is a nuclear protein expressed in all proliferating cells [32]. To compare the rate of cell proliferation, subcutaneous tumors were immunostained with anti-Ki67 antibody 42 days

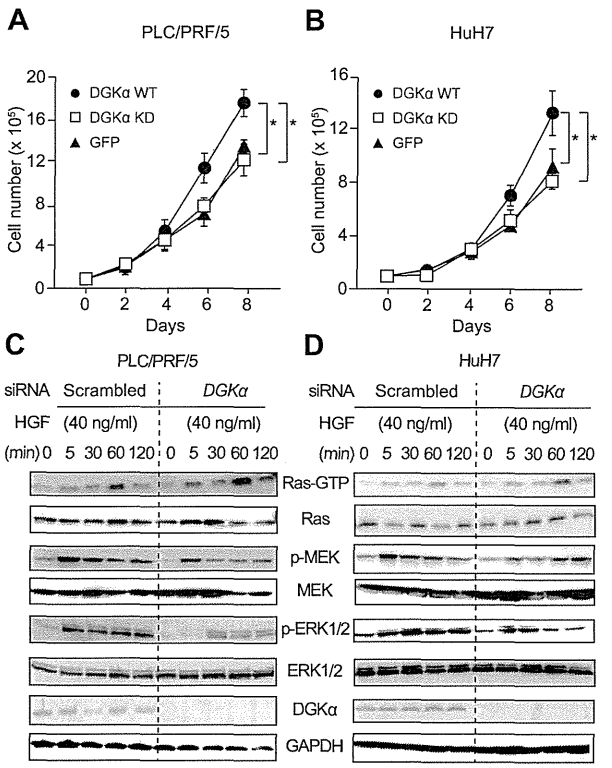


**Fig. 2. Effect of DGKα overexpression on HCC cell proliferation and impaired activation of MAPK signaling in DGKα-silenced HCC cells following HGF stimulation.** At the indicated times after transfection, (A) PLC/PRF/7 and (B) HuH7 cells were counted. Data shown are representative of at least three experiments. Asterisks (*) indicate statistical significance between cells transfected with WT DGKα and GFP alone or KD DGKα. (C and D) Ras–GTP precipitated with GST–Raf–RBD and total Ras, phosphorylated-MEK1/2 (p-MEK1/2), total MEK1/2, total ERK, phosphorylated-ERK1/2 (p-ERK1/2) and DGKα in cell lysates were detected by Western blotting. Downregulation of p-MEK1/2 and p-ERK1/2, but not Ras–GTP in DGKα-silenced HCC cells at all times after HGF stimulation.

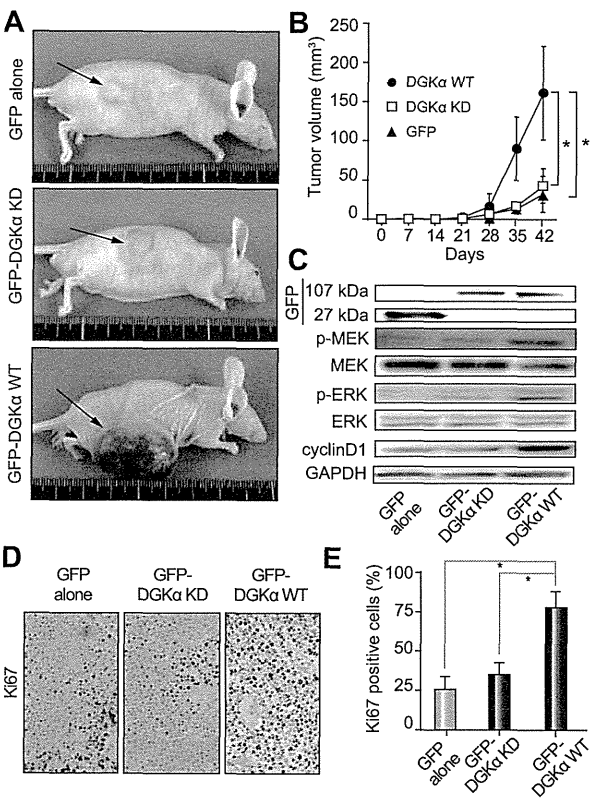


**Fig. 3. Effect of DGKα on *in vivo* growth of PLC/PRF/5 cell-derived tumors.** GFP alone, GFP–WT DGKα, or GFP–KD DGKα stable cell lines were injected subcutaneously into nude mice. (A) Forty-two days after injection, tumors were photographed. (B) Tumor growth was monitored for 42 days. (C) Phosphorylated-MEK (p-MEK) 1/2, total MEK1/2, phosphorylated-ERK (p-ERK) 1/2, total ERK, and cyclin D1 were detected. (D) Tumor samples were subjected to immunohistochemistry using Ki67 (400 × magnification). (E) Cell numbers positive for Ki67 are shown as mean ± S.D. Asterisks (*) indicate the statistical significance between tumors overexpressing WT DGKα and tumors overexpressing GFP alone or KD DGKα.

after injection with stably-expressing tumor cell lines. Tumors with overexpressed WT DGKα had significantly higher levels of Ki67 than those expressing GFP alone or KD DGKα (77% *vs.* 27% or 33%, respectively; $p < 0.05$) (Fig. 3D and E). DGKα activated MAPK signaling, and positively regulated cell proliferation in HCC *in vivo* models, which correlated with the results observed in *in vitro* models.

*High DGKα expression in HCC is a risk factor for recurrence after hepatectomy*

Western blot analysis showed that DGKα was detected at higher levels in cancerous tissues from surgical samples than in adjacent non-cancerous tissues (Fig. 4A). DGKα expression was immunohistochemically examined in 95 HCC resected tissue samples. Normal bile duct cells showed specific DGKα expression and were used as the internal positive control in all cases. DGKα immunoreactivity in cancer cells was observed in the cytoplasm and partially in the nucleus; however, hepatocytes from matched adjacent non-cancerous tissues were negative for DGKα immunoreactivity (Fig. 4B). The 95 cases were divided into two groups: a high DGKα expression group (n = 17) with ⩾20% of cancer cells staining positively for DGKα, and a low DGKα expression group with <20% cancer cells staining positively for DGKα. Table 1 shows a comparison of the clinicopathological factors between the high and low DGKα expression groups. There were no significant differences in clinicopathological factors between the two groups. Ki67 was also detected in the nuclei of cancer cells but not in corresponding non-cancerous tissues (Fig. 4B). The high DGKα expression group had significantly more positive Ki67 staining than the low DGKα expression group (11% *vs.* 3.7%; $p < 0.05$) (Fig. 4C). Phosphorylated-ERK1/2 expression was also detected in cancer cells but not in adjacent non-cancerous tissues (Fig. 4B); however, it could not be compared with DGKα expression by immunohistochemistry because it was expressed at low levels (12/95; 12%). Disease-free survival after hepatectomy was compared between the two groups; the disease-free survival rates of the low DGKα-expressing patients (59% at 3-year and 47% at 5-year) was significantly better than that of high-expressing patients (48% at 3-year and 18% at 5-year) ($p = 0.033$; Fig. 4D).